Development of microparticles incorporating chondroitin sulphate for application as Pickering stabilisers for topical applications

Maria Clara de Morais

The thesis presented to the

Escola Superior de Tecnologia e Gestão - Instituto Politécnico de Bragança

to obtain a master's degree in

Chemical Engineering

Within the context of the double diploma with

Universidade Tecnológica Federal do Paraná Campus Francisco Beltrão

Supervisors

Profª. Dra. Filomena Barreiro

Dra. Arantzazu Santamaria-Echart

Profª. Dra. Elisângela Düsman

Bragança, Portugal

2024

This work was partially supported by national funds through FCT/MCTES (PIDDAC) (CIMO, UIDB/00690/2020 (DOI: 10.54499/UIDB/00690/2020) and UIDP/00690/2020 (DOI: 10.54499/UIDP/00690/2020); and SusTEC, LA/P/0007/2020 (DOI: 10.54499/LA/P/0007/2020)), Fundação Araucária and Universidade Tecnológica Federal do Paraná within the context of the project PD&I Nº 429/2022, and Conselho Nacional de Desenvolvimento Científico e Tecnológico (CNPq#305029/2022-3).

ACKNOWLEDGMENTS

I would like to express my deep gratitude to everyone present during my academic journey, whether directly or indirectly. I would like to thank my family, especially my mother, Edicione Xavier de Morais, who has always been my greatest supporter, haven, and shelter throughout my life, not just during this period. To my father, Márcio Rogério de Morais, and my brother, João Pedro Xavier de Morais, for always supporting me and making me smile in the most difficult times. To my partner, Jean Almeida, for all his encouragement, affection and care, even at a distance.

To my supervisors, Prof. Dr Maria Filomena F. Barreiro, Dr Arantzazu Santamaria-Echart and Prof. Dr Elisângela Düsman, my most sincere thanks for the opportunities, teachings for guidance and patience throughout the development of this work. I would also like to thank my dear laboratory colleague, Tatiana La Banca Schreiner, for playing a fundamental role in the realisation of this work and for making this process lighter.

To the friends I met in Bragança, Helena Swiech, Júlia Matté and Sofia Bernardoni, thank you for the moments of laughter and for being by my side in times of anguish. To my colleagues in the lab, thank you for your willingness to help whenever I asked. Without all these people, this dream wouldn't have come true and I certainly wouldn't be who I am today. Thank you so much for being by my side.

ABSTRACT

Pickering emulsions, stabilised by solid particles, have been gaining prominence as an alternative to traditional surfactants and stabilisers, giving products of greater stability and unique characteristics. In this study, chitosan-based particles incorporating chondroitin sulphate were developed to produce Pickering emulsions for topical applications, followed by characterising the stabilising particles and the emulsions. For particle dispersion, size and distribution (DLS (dynamic light scattering)), stability (zeta potential (**ζ**)), and wettability (contact angle (θ)) were characterised. The emulsions' type, droplet size and distribution (DLS), stability (zeta potential and creaming index (CI)), colour, rheological properties, antioxidant activity, toxicity, cytoprotection and skin corrosion were assessed. In preliminary tests, relatively large and uniform particles were obtained, identifying the most promising formulations and the most compatible oil. The particles showed good stability, demonstrated by zeta potential values above 30 mV ($\zeta = 32.30 \pm 1.64$ mV), indicating good electrostatic repulsion and colloidal stability. In addition, they exhibited relative hydrophobicity, evidenced by a contact angle greater than 90° ($\theta = 97.10 \pm 2.91°$), characterising a moderately hydrophobic surface. Two emulsions were prepared: a base emulsion and another with the addition of vitamin E. Both were identified as O/W (oil/water) emulsions, characterised by the aqueous phase being continuous. These emulsions remained stable for 30 days, without phase separation, showing controlled droplet growth and pseudoplastic behaviour in the rheological tests, properties of a gel-like material in the amplitude and frequency analysis. In addition, the vitamin E emulsion showed high antioxidant activity throughout the study period. The emulsions had a light green colour characteristic of olive oil, with no toxicity or cytoprotective properties.

Keywords: Particles, Chondroitin Sulphate, Chitosan, Pickering Emulsions, Vitamins.

RESUMO

As emulsões de Pickering, estabilizadas por partículas sólidas, têm vindo a ganhar destaque como alternativa aos tradicionais tensioactivos e estabilizantes, conferindo aos produtos maior estabilidade e caraterísticas únicas. Neste estudo foram desenvolvidas partículas à base de quitosano incorporando sulfato de condroitina para a produção de emulsões Pickering destinadas a aplicações tópicas, seguindo-se a caraterização das partículas estabilizadoras e das emulsões. Para a dispersão das partículas, foram caracterizados o tamanho e respetiva distribuição (DLS (dynamic light scattering)), a estabilidade (potencial zeta (**ζ**)), a molhabilidade (ângulo de contacto (θ)). No caso das emulsões, foram avaliados o tipo de emulsão, o tamanho e a distribuição de tamanho das gotículas (DLS), a estabilidade (potencial zeta e creaming index (CI)), a cor, as propriedades reológicas, a atividade antioxidante, a toxicidade, a citoprotecção e a corrosão cutânea. Em testes preliminares, foram obtidas partículas relativamente grandes e uniformes, identificando as formulações mais promissoras e o óleo mais compatível. As partículas apresentaram boa estabilidade, demonstrada por valores de potencial zeta acima de 30 mV (ζ = 32,30 ± 1,64 mV), indicando uma boa repulsão eletrostática e estabilidade coloidal. Além disso, exibiram hidrofobicidade relativa, evidenciada por um ângulo de contato superior a 90° (θ = 97,10 ± 2,91°), caracterizando uma superfície moderadamente hidrofóbica. Foram preparadas duas emulsões: uma emulsão base e outra com a adição de vitamina E. Ambas foram identificadas como emulsões do tipo O/W (óleo/água), caracterizadas pela fase aquosa como contínua. Estas emulsões mantiveram-se estáveis durante 30 dias, sem separação de fases, apresentando um crescimento controlado das gotículas, e um comportamento pseudoplástico nos testes reológicos, propriedades de um material tipo gel na análise de amplitude e frequência. Adicionalmente a emulsão com vitamina E apresentou uma elevada atividade antioxidante durante todo o período de estudo. As emulsões apresentavam uma cor verde claro caraterística do azeite, sem toxicidade nem propriedades citoprotectoras.

Palavras-chave: Micropartículas, Sulfato de Condroitina, Quitosana, Emulsões Pickering, Vitaminas.

INDEX

1. MOTIVATION AND OBJECTIVES 13

1.1. Objective 13

1.2. Specific Objectives 14

2. BIBLIOGRAPHIC REVIEW 15

2.1. Microparticles 15

2.2. Polyelectrolyte complexes 15

2.3. Chondroitin Sulphate 16

2.4. Chitosan 18

2.5. Emulsions 19

2.6. Pickering Emulsions 20

2.7. Vitamins 22

3. METHODOLOGIES 23

3.1. Materials 23

3.2. Preparation of the polyelectrolyte complex 23

3.3. Preparation of the Pickering emulsions 24

3.4. Characterisation of the particles 25

3.5. Characterisation of the emulsions 26

3.5.1. Biologic activity 29

3.5.1.1. Cell culture 29

3.5.1.2. Cytotoxicity/Antiproliferative activity test 30

3.5.1.3. Cytoprotection/Photoprotection test 32

3.5.1.4. Skin Corrosion test *in vivo* 33

3.5.1.5. Statistical analysis 33

4. RESULTS AND DISCUSSION 34

4.1. Development of particle dispersion 34

4.2. Emulsions development 37

4.3. Development of the formulation for cosmetic applications 43

4.3.1. Dispersion characterisation 43

4.3.1.1. Particle size 43

4.3.1.2. Zeta potential 45

4.3.1.3. Contact angle 45

4.3.2. Emulsion characterisation 46

4.3.2.1. Emulsion type 47

4.3.2.2. Creaming Index 48

4.3.2.3. Droplet size 49

4.3.2.4. Zeta Potential 51

4.3.2.5. Colour test 52

4.3.2.6. Rheological properties 53

4.3.2.7. Antioxidant activity 56

4.3.2.8. Biologic activity 57

4.3.2.8.1. Cytotoxicity/Antiproliferative activity 57

4.3.2.8.2. Cytoprotection/ Photoprotection test..... 59

4.3.2.8.3. Skin corrosion test *in vivo* 62

5. CONCLUSIONS 66

5.1. Future Works..... 67

REFERENCES 68

INDEX OF FIGURES

Figure 1- Chemical structure of chondroitin sulphate 17
Figure 2- Chemical structure of chitosan..... 18
Figure 3- Emulsions O/W and W/O 19
Figure 4- Contact angle representation..... 21
Figure 5- Scheme of the polyelectrolyte complex formation process 24
Figure 6- Colorimeter 27
Figure 7- Rheometer 28
Figure 8- Cells NIH3T3 under a stereoscopic microscope..... 30
Figure 9- Radiation chamber used to carry out the experiments 31
Figure 10- Plate of NIH3T3 cells with diluted formazan crystals..... 31
Figure 11- Graphs of particle size distribution in number and volume for a) 1.6Ch_25CS, b) 1.6Ch_15CS, c) 1.6Ch_10CS, d) 1.6Ch_5CS, e) 0.8Ch_12.5CS and f) 0.4Ch_6.25CS 36
Figure 12- Destabilised emulsion 37
Figure 13- Appearance of Ep1.6Ch_5CS20/80 Pickering emulsion at 7 days..... 40
Figure 14- Creaming index - EAO1.6Ch_5CS and EAD1.6Ch_5CS 40
Figure 15- Creaming index - Study of the third stability study in the production of Pickering emulsions by Creaming index 41
Figure 16- Particle size distribution graph in number and volume sample 1.6Ch_5CS..... 44
Figure 17- Contact angle analysis at t=30s..... 46
Figure 18- Droplet test of the emulsion..... 47
Figure 19- Creaming index of EAO1.6Ch_5CS70/30 and VitE1.6Ch_5CS samples over 30 days. 48
Figure 20- Emulsion droplet size distribution graph in number and volume at t=0 for a) EAO1.6Ch_5CS70/30 and b) VitE1.6Ch_5CS 50
Figure 21- Emulsion droplet distribution graph over one month in volume for a) EAO1.6Ch_5CS70/30 and b) VitE1.6Ch_5CS. 51
Figure 22- Emulsions' viscosity in function of the shear rate 53
Figure 23- Rheological behaviour of the sample as a function of the shear strain..... 54
Figure 24- Rheological behaviour of the samples as a function of frequency 55

Figure 25- Antioxidant activity expressed as a percentage of radical scavenging activity (%RSA) for the VitE1.6Ch_5CS sample after production (t0) and after 30 days (t30)..... 56
Figure 26- Average absorbance of NIH3T3 cells treated for 24 and 48 hours with different concentrations for a) EAO1.6Ch_5CS70/30 and b) VitE1.6Ch_5CS..... 58
Figure 27- Mean absorbance and standard deviation of NIH3T3 cells treated with radiation intensities for 24h and 48h..... 60
Figure 28- Mean absorbance and standard deviation of NIH3T3 cells treated with 400 μL. mL^{-1} of the samples and UVB radiation alone and in simultaneous, pre-treatment, and post-treatment cytoprotection/photoprotection treatments..... 62
Figure 29- Effect observed under a stereoscopic microscope of sample EAO1.6Ch_5CS70/30 on the organism *E. fetida*..... 64
Figure 30- Effect observed under a stereoscopic microscope of sample VitE1.6Ch_5CS on the organism *E. fetida*..... 64
Figure 31- Corrosive effect observed under a stereoscopic microscope of the positive control sample (CO+) on the organism *E. fetida.*..... 65

INDEX OF TABLE

Table 1- Preparation composition of all dispersions..... 34
Table 2- Average particle diameter by volume of the particles' dispersion prepared through the third methodology 35
Table 3- Initial screening of Pickering emulsions production stability by Creaming index .. 38
Table 4- Creaming index of the Pickering emulsions prepared with the 1.6Ch_5CS dispersion. 39
Table 5- Stability study in the production of Pickering emulsions by Creaming index… 40
Table 6- Study of the third stability study in the production of Pickering emulsions by Creaming index …… 41
Table 7- Particle size distribution in volume for the sample 1.6Ch_5CS..... 43
Table 8- Particle size distribution in number for the sample 1.6Ch_5CS... 44
Table 9- Droplet size of emulsions for the t=0 and t=30. 49
Table 10– ζ of the emulsions 52
Table 11- Colour test of the emulsions..... 53
Table 12- Percentage viability of NIH3T3 cells, MTT test for both samples. 57
Table 13- Percentage viability of NIH3T3 cells treated with different radiation intensities for 24h and 48h, using the MTT test..... 59
Table 14- Percentage viability of NIH3T3 cells submitted to treatment with a concentration of 400 μL. mL^{-1} for the samples and UVB radiation alone and in cytoprotection/photoprotection treatments of the simultaneous (SIM), pre-treatment (PRE), and post-treatment (POST) types 61
Table 15- Average percentage of worms and an average number of changes in worms exposed to the treatment solutions for 2h and 24 h 63

LIST OF ABBREVIATIONS

Ch	Chitosan
CI	Creaming index
CO-	Negative control group
CO+	Positive control group
CS	Chondroitin sulphate
DD	Degree of deacetylation
DLS	Dynamic light scattering
DMEM	Dulbecco's Modified Eagle Medium
DMSO	Dimethy
DMSO	Dimethylsulphoxide
DPPH	2,2-diphenyl-1-picrylhydrazyl
G ‘	Elastic modulus
G”	Viscous modulus
GHS	Globally Harmonised System of Classification and Labelling of Chemicals
IC_{50}	maximum inhibitory concentration
MMS	Cytotoxic agent methyl methanesulphonate
O/W	Oil/water
PBS	Phosphate-buffered saline
PBS	Phosphate-buffered saline
PC	Polyelectrolyte complex
PCs	Polyelectrolyte complexes
UVB	Ultraviolet rays B
UVR	Ultraviolet Radiation
VC	Cell Viability
W/O	Water/oil
3D	Three-dimensional
θ	Contact angle
ζ	Zeta potential

1. MOTIVATION AND OBJECTIVES

This work is part of the project ‘Obtenção, caracterização e avaliação do potencial bioativo de sulfato de condroitina extraído de escamas de tilápia’ at UTFPR's Francisco Beltrão campus. This study adopts an ecological approach by seeking a possible application for this waste, contributing to the valorisation of industry by-products and reducing environmental impacts.

At the same time, the use of emulsions in the development of pharmaceutical and cosmetic products has gained prominence, especially Pickering emulsions, which are stabilised by solid particles. These emulsions have greater thermal stability and are partially dispensed with the use of synthetic surfactants, reducing environmental impacts and improving functional characteristics. In this context, particles derived from bioactive materials, such as chondroitin sulphate (CS), can play a dual role: acting as ecological stabilisers and offering additional bioactive properties, such as greater solubility, stability and bioavailability. The project therefore aims to explore the potential CS fate not only as a sustainable by-product but also as an innovative component for emulsion applications.

1.1. Objective

This study aims to develop and evaluate the formation and stability of chitosan (Ch) particles incorporating CS and to characterise them to produce Pickering emulsions envisaging topical applications.

1.2. Specific Objectives

This work has the following specific objectives:

- The selection of the methodology to be used through a bibliographic revision;
- The production of Ch-based particles and the incorporation of CS;
- The characterisation of the produced particles;
- Development and optimisation of stable Pickering emulsions, with and without vitamin E;
- Characterisation and biological activity of the produced emulsions.

2. BIBLIOGRAPHIC REVIEW

2.1. Microparticles

Microparticles are spherical particles with a diameter ranging from 1 to 1000 µm. These particles can be manufactured by different methods, using natural or synthetic materials. This allows for the formation of various types of particles in terms of size, distribution, composition, surface chemistry, topography and morphology (CAMPOS et al., 2013; KAWAGUCHI, 2000).

In terms of their structure, microparticles can be divided into microcapsules and microspheres. Microspheres are characterised by their active compound being homogeneously dissolved in a material matrix, while microcapsules have a core with all the active compounds concentrated inside it. This core can be solid, liquid, or even gaseous (CAMPOS et al., 2013).

Nanoparticles and microparticles can be used in a variety of applications because they differ not only in size but also in their crystallisation, solubility, melting point, glass transition temperature, dissolution, and other properties (DA SILVA et al., 2023; OTTO; OTTO; DE VILLIERS, 2015). The larger microparticles can give them an advantage over nanoparticles; particles larger than 100 µm have a better skin retention profile (DWIPAYANTI et al., 2022).

Particular polymeric particles, microparticles, are widely used in various applications, such as cosmetic products, drug delivery, tissue engineering, multiplexed biosensors, paints, fillers, and building blocks for self-assembly, among others (GANGULY et al., 2021; MORATILLE et al., 2022). The cosmetics industry attributes several functionalities to microparticles in various products, from essential care products to repellents (ROCHA et al., 2021). Polyelectrolyte complexes are responsible for the stability of the aqueous phase and gels in these products (MAYILSWA; BONEY; KANDASUBRAMANIAN, 2022).

2.2. Polyelectrolyte complexes

Polyelectrolytes are polymers charged with negative and/or positive charges, and their categorisation is based on their origin, type of charge, composition, and location of their

charges. These ionic polymers have diverse properties due to their flexibility and electrostatic interactions (CHAKRABORTY; BHATTARAI; DE, 2022). This type of polymer can form a polyelectrolyte complex (PC) through a mixture of two or more similar polyelectrolytes with opposite charges and in solution. It is important to emphasise that the molecular properties of the complexes are directly linked to the used polymers and the formation conditions (DU et al., 2008; BEDIAKO et al., 2023).

Polyelectrolyte complexes (PCs) are relatively easy to synthesise, and in recent years, these complexes have been increasingly studied for the transport of medicines. PCs formation generally involves two or three steps (MEKA et al., 2017). The first stage is the complex formation, which is characterised by being instantaneous and can lead to distortions in the polymer chain. The next stage involves rearranging the chains, leading to the formation of new bonds. The last stage consists of joining various complex entities, probably by hydrophobic interactions, resulting in tangled aggregates, fibrils, and ordered networks (BEDIAKO et al., 2023).

The polymer's nature directly influences the characteristics and structure of the PCs, the mixing ratio, the ionic strength, and the temperature (FERREIRA; ZUCOLOTTO, 2024). These complexes also have high mechanical strength, excellent thermal stability, and biocompatibility (BEDIAKO et al., 2023).

2.3. Chondroitin Sulphate

CS comprises D-glucuronic acid and N-acetyl-D-galactosamine and is considered a linear anionic glycosaminoglycan found in extracellular matrices, as shown in Figure 1 (HAN et al., 2023). This compound is present in mammals and invertebrates. It plays an extremely important role in biological processes, acting as a regulator of growth factors, cytokines, chemokines, adhesion molecules, and lipoproteins through the ligands of these proteins (MALAVAKI et al., 2008).

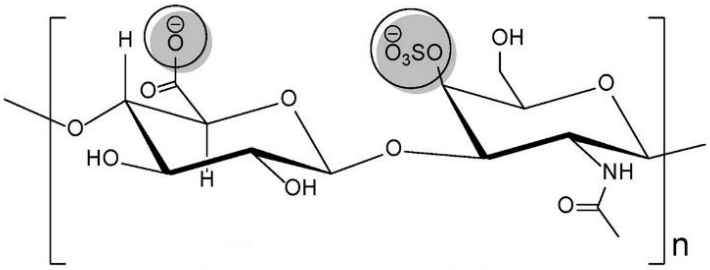

Figure 1- Chemical structure of chondroitin sulphate. Adapted from SHARMA et al. (2019)

The CS has an inflammatory action, presenting potential in applications such as the treatment of osteoarthritis. Other properties include antiviral action, anti-infective action, regeneration, and tissue engineering (SCHIRALDI; CIMIDI; DE ROSA, 2010). The first test to isolate CS was carried out in 1884, and it was removed from cartilaginous tissues. However, this study did not establish which monosaccharides formed this compound and how. It wasn't until 1925 that Levene first elucidated CS composition (JARDIM, 2013).

The first CS extraction studies used alkaline treatments for protein catabolism in tissues. However, these treatments resulted in the degradation of sulphate groups (MEYER; ODIER; SIEGRIST, 1948). Therefore, it was necessary to develop new methods, such as using CaCl. Although this method takes longer, it dissolves the collagen without degrading the CS (BLIX; GARDELL, 1960).

The first step in any CS extraction is the preparation of the extracellular matrices to clean this structural material, which is then boiled in water for 10 minutes at 90-95 °C to remove the adhered flesh and connective tissues. These tissues are usually associated with muscles, and glycosaminoglycans are bound to proteins, which makes extraction even more difficult. Therefore, most of the extraction techniques include proteolytic digestion of the proteoglycans and the purification of the sulphate, varying mainly in temperature, pH, enzyme concentration, and reaction time according to the type of tissue (JARDIM, 2013).

2.4. Chitosan

Ch is obtained by alkaline deacetylation of the natural polymer chitin (CHOI et al., 2024), mainly found in the exoskeletons of crustaceans and insects and even in the cell walls of some fungi. This macromolecule is considered a cationic polysaccharide and comprises glucosamine and N-acetylglucosamine units, as illustrated in Figure 2. In addition, this polymer can be differentiated by its molecular weight, impurity content, and deacetylation degree (DD), ranging from 50 to 95%, depending on the source and the preparation method (LUNKOV et al., 2023; JARDIM, 2013).

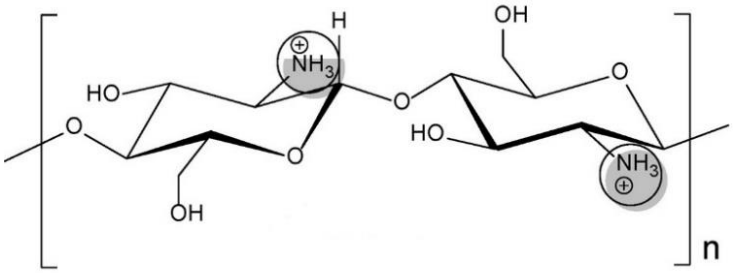

Figure 2- Chemical structure of chitosan. Adapted from SHARMA et al. (2019)

DD is a chemical parameter that expresses the average content of acetylated residues in the Ch chains. This variable can influence other chemical, physical, and biological parameters, including hydrophobicity, cross-linking capacity in the presence of specific cross-linking agents, solubility, and viscosity in solution (JARDIM, 2013).

Among this polysaccharide's potential chemical and biological properties, its antimicrobial activity, biodegradability, biocompatibility, lack of toxicity, ability to absorb metals and form membranes, and hemostatic power are considered (MARTINS, 2013). The impact of the molecular weight of this polymer is also a determinant factor of the biological, mechanical, and physical-chemical properties applicable in certain areas (CHOI et al., 2024).

Due to the free NH groups' protonation in the deacetylated units, Ch is soluble in acidic aqueous solutions. This solubility only occurs at pH values below 6.2 (MARTINS, 2013), and

the most commonly used acids for solubilising are acetic, formic, and citric acid (JARDIM, 2013).

2.5. Emulsions

Emulsions are formed by the dispersion of at least two liquids. They are classified by the size of their droplets: nanoemulsions (0.05-0.5 μm), microemulsions (0.01-0.1 μm), and coarse emulsions (>0.5 μm). Microemulsions are more thermally stable due to their low interfacial tension (BURGUESA; BURGUESA, 2012). Another way of classifying emulsions is according to the dispersion phase: oil in water (O/W) and water in oil (W/O) (LI et al., 2024). In O/W emulsions, the dispersed phase is the oil, and the continuous phase is the water, while the opposite consists of W/O emulsions (ZANOTTI, 2017), as shown in Figure 3.

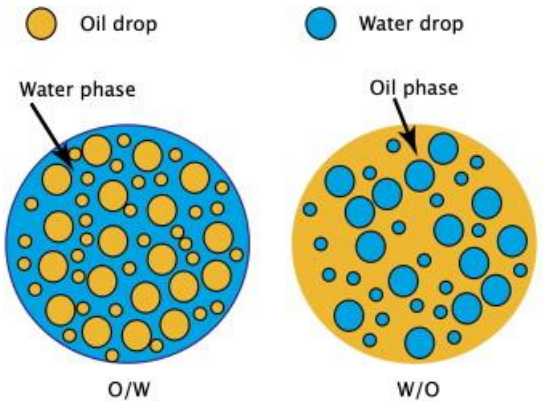

Figure 3- Emulsions O/W and W/O. Adapted from MARTÍNEZ-PALOU et al. (2011).

The conventional emulsions are thermodynamically less stable systems, i.e., they can undergo destabilisation phenomena such as gravitational separation, flocculation, coalescence, and Ostwald ripening. Emulsions, therefore, need stabilisers, such as surfactants, polymers, or amphiphilic particles. These stabilisers are adsorbed at the O/W interface, increasing stability through electrostatic repulsion, steric hindrance, or both (SU et al., 2024).

One of the main applications of emulsified systems is in the pharmaceutical field as carriers of polar and apolar drugs (CASTRO, 2014). In addition, the targeting of this drug is

linked to the droplets' size and distribution. Smaller droplets tend to provoke fewer inflammatory reactions and immune responses as they remain in circulation longer and have a greater capacity to bind and accumulate in the desired location. For treatments that require greater control over the release of the dose, emulsions with homogeneous droplets (monodisperse) are used (DOS SANTOS, 2011).

Another area that has received a lot of attention is nutraceuticals, where foods have more functional attributes than conventional foods. Including these foods in a diet can regulate the body's functions and help prevent hypertension, diabetes, cancer, osteoporosis, and coronary heart disease (MORAES, 2006). Another field widely studied is cosmetics and personal care products, as emulsions can form lamellar structures that increase skin hydration (TOPAN, 2012).

2.6. Pickering Emulsions

Typically, surfactants and organic compounds stabilise classical emulsions, while solid particles are used in Pickering emulsions. The most apparent difference between the classical and Pickering emulsions is their stabilisation. In conventional emulsions, the system's stability is achieved by the absorption of amphiphilic compounds, which modify the interfacial characteristics of the two phases. However, in Pickering emulsions, the absorption of the stabilising particles occurs between the interface of the liquids, creating a physical barrier and limiting the coalescence between the droplets (RAMSDEN, 1903). These emulsions establish a direct relationship between the energy of the droplet's formation and the particles (LOW et al., 2020), as described by Equation 1 (BRIGGS, et al., 2018).

$$E = \pi R^2 \gamma_{Ow} (1 \pm cos\theta)^2 \quad (1)$$

Where: R= particle radius

γ_{Ow}= interfacial horniness

θ= contact angle

E= energy to adsorb or desorb particle

The stability of a Pickering emulsion is determined by the wettability and size of the particles (ORTIZ et al., 2020). The wettability is represented by the contact angle between the O/W interphase and is essential to determine if it is prone to form O/W or W/O. In O/W emulsions, the particles typically present a hydrophilic character, resulting in a contact angle of less than 90°, while hydrophobic particles have an angle greater than 90°, forming W/O emulsions (GRAMATGES, 2018). The contact angle is illustrated in Figure 4.

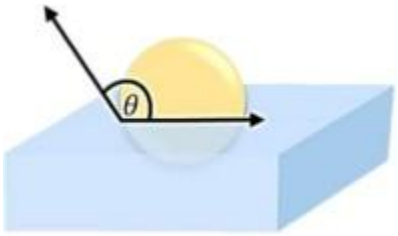

Figure 4- Contact angle representation. Adapted from GRAMATGES (2018).

Pickering emulsions comprise an aqueous phase, an oily phase, and solid particles. These components can be homogenised by high pressure, rotor-stator, or membrane emulsification. High-pressure emulsification is a continuous mixing method that uses high-pressure pumps and homogeneous nozzles (BELTRÁN et al., 2022). This method has advantages such as the ability to process large volumes, obtain very small droplets, and adjust droplet size or the number of homogenisation cycles. It is used at the industrial level but also presents some disadvantages, such as high operating costs, the risk of particle degradation, the need for a minimal volume, and difficulties in cleaning (KÖHLER et al., 2010).

The rotor-stator method has several advantages, such as low operating costs, ease of assembly, a speedy process, the need for a small operating volume, and specific types of rotor-stator conformations to particular needs (ALBERT et al., 2019; BOT et al., 2013). However, some disadvantages include the possibility of sample non-uniformity, risk of temperature rise, energy consumption, wide droplet distribution, and high shear rate (ALBERT et al., 2019, THOMPSON et al., 2011).

In the membrane emulsification method, the solid particles are slowly adsorbed between the two immiscible phases with controlled shear conditions and injection speed (MANGA et al., 2012). The advantages of this technique include their suitability for products with sensitivity to shear stress, producing small, uniform emulsion droplets of low polydispersity, low operating costs, and no heating effects during production (YUAN et al., 2009; THOMPSON; ARMES; YORK, 2011). However, this method can only be carried out on low-viscosity systems and takes time (SUN et al., 2014; YUAN et al., 2009).

2.7. Vitamins

The emulsions used in cosmetics demand extremely strict standards regarding texture, consistency, colour, fragrance and other aspects. Due to these requirements, the formulation of these emulsions is complex, as it includes various components, such as vitamins, fragrances, preservatives, oils, water, surfactants and colourants. Each of these ingredients plays a specific role in the properties of the emulsion, and it is essential to consider both the individual characteristics and the possible interactions between them (TERESCENCO et al., 2018).

In addition to cosmetic emulsions, other systems were used to incorporate vitamins, such as multicomponent emulsions, which are widely used in everyday life for the controlled release of medicinal components and nutrients, including vitamins. Encapsulation can enable these developments (MINAKOV et al., 2022). Among these vitamins, vitamin E is used extensively in various industrial preparations, covering the pharmaceutical, cosmetic and food industries (YANG; MCCLEMENTS, 2013).

Vitamin E was discovered in 1922 by Evans and Bishop (EVANS; BISHOP, 1922). Over the century, it has been proven that this vitamin is essential for body development and the health of living beings, acting as a powerful antioxidant and free radical scavenger in food and industrial products (NOGUCHI; NIKI, 2024; NIKI, 2021). Vitamin E is composed of a 6-hydroxychrome ring with a side chain and is made up of a group of four tocotrienols and four tocopherols, known as α, β, γ and δ-tocopherols (NIKI, 2021).

3. METHODOLOGIES

3.1. Materials

Chitosan (with a degree of deacetylation of 90% and a density of 8.5 mPa.s, according to the supplier, Biolog, Germany). Acetic Acid (Honeywell/Fluka, Spain). Chondroitin Sulphate (soluble in water, according to the supplier, SM Emprendimentos Farmacêuticos LTDA, Brazil). Distilled water. Miglyol 812 (Acofarma, Spain). Virgin Olive oil (Fagron, Spain). DL-α-Tocopherol97+% (Thermo Scientic, Germany).

3.2. Preparation of the polyelectrolyte complex

The particle preparation method followed the work of FARJADO et al. (2010) with adaptations. The Ch solution was prepared using an acetic acid solution (100 mL) with a concentration of 0.1 M and 1.6 g of powdered Ch. This solution was stirred for 2 hours on a stirring plate. The CS solution was prepared with distilled water, using 5 g of CS in 100 mL. Both solutions had a volume of 100 mL, resulting in a significantly higher proportion of CS. The CS solution was added to the Ch solution using a peristaltic pump (ISM596B, Ismatec SA, Switzerland) at a flow rate of 6.4 $mL.min^{-1}$. The solution was then left to stabilise for 24 hours (h). Figure 5 shows this process schematically.

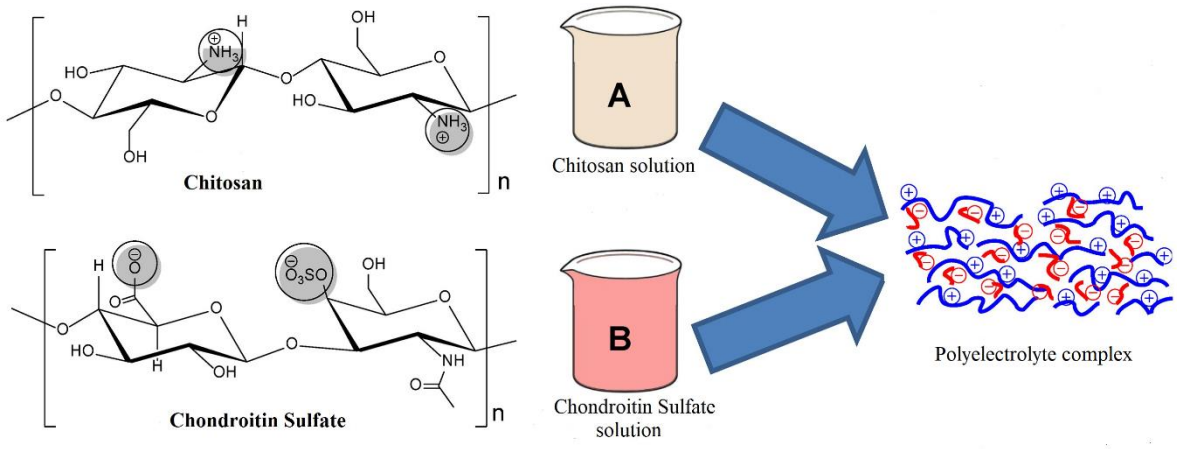

Figure 5 – Scheme of the polyelectrolyte complex formation process. Adapted from SHARMA et al. (2019)

3.3. Preparation of the Pickering emulsions

The Pickering emulsions were prepared following the methodology of GHIRRO (2020), with some adaptations. The emulsions were formulated using an O/W ratio of 70/30, for a total volume of 50 mL. A pre-homogenisation stage was initially carried. To do this, a peristaltic pump (ISM596B, Ismatec SA, Switzerland) with a flow rate of 6.4 mL.min-¹ was used in conjunction with a stirring plate (VWR, USA), allowing the oil phase to be added slowly and continuously in the particles' aqueous solution. Then, the mixture was homogenised using an Ultra-turrax (Unidrive X1000 Homogeneizer Drive CAT Scientific, Germany) for 5 minutes at 13500 rpm.

Emulsions containing vitamin E were also prepared. To this, 1% of alpha-tocopherol was incorporated into the oil phase and homogenised using a vortex for 2 minutes. The preparation procedure was similar to the one used for the base emulsions.

3.4. Characterisation of the particles

The emulsion characterisation comprised the determination of size and distribution, stability and wettability. Particle size and respective distribution are crucial factors in the preparation of the emulsions and are used as quality parameters of the final product.

The dynamic light scattering (DLS) technique is widely used to assess the particle size ranging from 1 to 1000 nm, using the light scattering. A Mastersizer 3000 equipment (Malvern Instruments, United Kingdom) was employed, using a refractive index of 1.662 for the analysis. Five consecutive measurements were taken for each sample at room temperature and the values of D_{10}, D_{50}, D_{90}, which were determined both in volume and number, and $D_{4;3}$and Span was determined in volume.

The stability of the dispersion was assessed using the electrostatic repulsion force, quantified by the zeta potential (ζ) generated by the particles. Three consecutive measurements were carried out at room temperature using the ZetaSizer Ultra equipment (WR14 1XZ UK, Malvern Instruments, United Kingdom).

The wettability of the particles was analysed to determine their hydrophilic or hydrophobic character. The contact angle (θ) is essential to decide on the type of emulsion to be formed (SHARKAWY et al., 2020). For this analysis, an optical contact angle measuring device (OCA15 plus, Germany) was used, and 50 g of the dispersion was placed in a Petri dish, which was allowed to dry at room temperature until a film was formed. The film was placed on a platform, and 4 µL of deionised water was injected using a high-pressure injector. During the analysis, a digital camera attached to the equipment recorded images of the droplets. The contact angles were calculated using the equipment's software based on the Laplace-Young equation (Equation 2).

$$\Delta p = 2\gamma H \quad (2)$$

Where: Δp = pressure variation

γ = interfacial tension

H = surface curvature

3.5. Characterisation of the emulsions

Determining the emulsion type is an important parameter to assess the potential use of the emulsion. The emulsion type was classified using the droplet test following the method described by LV et al. (2020). In this procedure, an emulsion droplet was added to a beaker containing pure water and another containing oil. If the drop solubilised quickly in water, the emulsion was classified as O/W. If the drop was solubilised in oil, the emulsion was classified as W/O.

The creaming index (CI) is an essential parameter for an emulsion's stability over time. This analysis quantifies the phase separation of an emulsion, a common phenomenon in unstable emulsions. It is calculated using Equation 3.

$$CI = \left(\frac{H_S}{H_T}\right) * 100 \quad (3)$$

Where: CI= creaminess index

H_s= height of serum phase

H_T= total height

The size and distribution of the droplets can influence properties such as stability, viscosity and bioavailability, among others. DLS analysis was performed using laser diffraction equipment (Mastersizer 3000, Malvern Instruments, United Kingdom).

The stability of an emulsion is directly related to the ζ, as this parameter is crucial for preventing coagulation and maintaining colloidal stability. Therefore, the ζ value of the emulsion was used to quantify its stability. Three consecutive measurements were carried out at room temperature using the ZetaSizer Ultra equipment (WR14 1XZ UK, Malvern Instruments, United Kingdom).

The colour analysis was carried out according to the methodology of GHIRRO (2020) using a colourimeter (Model CR-400, Konica Minolta Sensing Inc., Japan) equipped with a

support accessory and a sample container. The results were expressed by the International Commission on Illumination (CIELAB) using “L*” (luminosity (lightness and darkness), “a*” (redness and greenness) and “b* (yellowness and blueness). The measurements were carried out in triplicate. Figure 6 shows the used equipment model.

Figure 6 - Colorimeter. From KONIKA MINOLTA (2024)

The rheological behaviour of the emulsions was determined using a rheometer (NETZSCH, Gerätebau GmbH, Germany). The measurements were made using a 20 mm diameter parallel plate with a fixed aperture of 1 mm. For the dynamic and static rheological analyses, the following analysis were performed: a viscosity curve as a function of shear rate, with a variation from 0.1 to 1000 s^{-1}; an amplitude curve, with a variation in shear stress in the range from 0.01 to 100%; and a frequency curve, with a variation from 0.1 to 10 Hz. Figure 7 shows the used rheometer.

Figure 7 – Rheometer. From INDUSTRY PLAZA (2024)

To verify the effectiveness of incorporating alpha-tocopherol, the antioxidant activity of the emulsion was analysed and monitored over 30 days through DPPH (2,2-diphenyl-1-picrylhydrazyl) assays. The emulsions were diluted 50, 100, 500 and 1000 times using an 80% (v/v) methanol aqueous solution. Then, 30 µL of the diluted samples were transferred to a 96-well microplate and mixed with 270 µL of methanolic DPPH solution (6×10^{-5} mol.L-¹). The plate was incubated at 37 °C for 60 minutes in the dark. DPPH reduction was measured by determining the absorbance at 517 nm using a microplate reader (BIOTEK, USA). After the measurements, the radical scavenging activity (RSA) was calculated by the percentage of DPPH decolourisation using Equation 4.

$$\%RSA = \left[\frac{Abs_{control} - Abs_{sample}}{Abs_{control}}\right] * 100 \quad (4)$$

Where: $\%RSA =$ percentage DPPH decolourisation

$Abs_{control}$= control absorbance

Abs_{sample}= sample absorbance

The results were expressed in terms of maximum inhibitory concentration (IC_{50}), corresponding to the sample concentration needed to reduce the initial concentration of DPPH radical by 50%.

3.5.1. Biologic activity

It is essential to check the safety of cosmetic emulsions to ensure their compatibility with the skin and avoid adverse reactions such as irritation or sensitisation. In this context, studies were conducted to characterise the biological activity of the samples, including toxicity tests, UV radiation protection tests and skin interaction analyses using live earthworms as a biological model.

3.5.1.1. Cell culture

The biological tests on the NIH3T3 cells were carried out at the UTFPR Francisco Beltrão campus. NIH3T3 cells, fibroblasts derived from *Mus musculus* embryonic tissue, were grown in 25 cm^2 culture flasks containing 10 mL of Dulbecco's Modified Eagle Medium (DMEM) culture medium, supplemented with 10% foetal bovine serum and incubated at 37 °C with 5% carbon dioxide (CO_2). The cells were obtained from the Banco de Células do Rio de Janeiro. Figure 8 shows the cells used under a stereoscopic microscope.

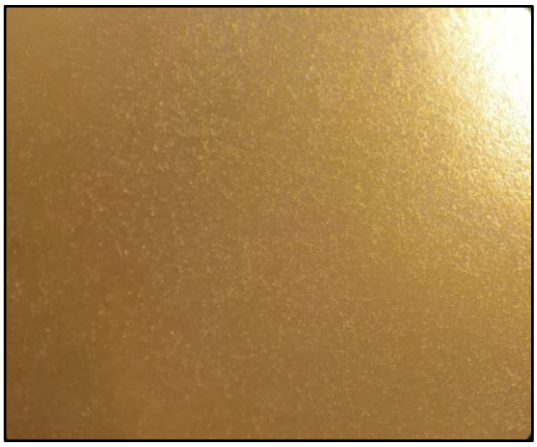

Figure 8 - Cells NIH3T3 under a stereoscopic microscope.

3.5.1.2. Cytotoxicity/Antiproliferative activity test

The MTT test was carried out according to the protocol suggested by MOSMANN (1983) to check cell viability with modifications. NIH3T3 cells were cultured at a density of $1x10^4$ cells per well in 96-well plates with 100 µL of culture medium supplemented with 10% foetal bovine serum for 24h.

After the cells had stabilised, the culture medium was discarded and then supplemented culture medium containing the following treatments was added: negative control, positive control and the treatments with the samples at concentrations of 1, 5, 10, 50, 100, 200, 300, 400, 500 and 1000 µL.mL-¹. The negative control group (CO-) contained only cells and supplemented culture medium. The positive control group (CO+) contained cells and the cytotoxic agent methyl methanesulphonate (MMS - 150 µM diluted in supplemented culture medium).

For the Ultraviolet rays B (UVB) radiation treatments, after stabilisation, the culture medium was removed and replaced with 20 µL of PBS (phosphate-buffered saline) in each well. In a radiation chamber, the cells were exposed to UVB radiation (30, 60 and 90 mJ.cm-2). Immediately after exposure, a new supplemented culture medium was added to the wells.

The radiation chamber was designed and built to the dimensions that showed the most uniform radiation intensity values (35 x 10 x 40 cm, depth x width x height). It has an internal aluminium coating that allows for uniform light intensity, as suggested by RANDIVE (2016). The radiation is supplied by a lamp with a wavelength between 280 - 315 nm, which comprises

UVB radiation, and with 8W of power. To monitor Ultraviolet Radiation (UVR) intensity, there is an Arduino circuit using the ml8511 sensor, which captures waves in the 280 - 390 nm range and delivers reading results in $mW.cm^{-2}$. Figure 9 shows the chamber used.

Figure 9 - Radiation chamber used to carry out the experiments.

After treatment with the creams or radiation, the plates were incubated for 24h and 48h, and after each period, the treatment was replaced with culture medium plus MTT (0.167 $mg.mL^{-1}$). The plates were incubated for another four hours, and the medium with MTT was replaced with 100 µL of dimethylsulphoxide (DMSO) to solubilise the formazan crystals. The absorbance was read on a microplate reader (Thermo Plate) at 492 nm. Figure 10 shows the plate used.

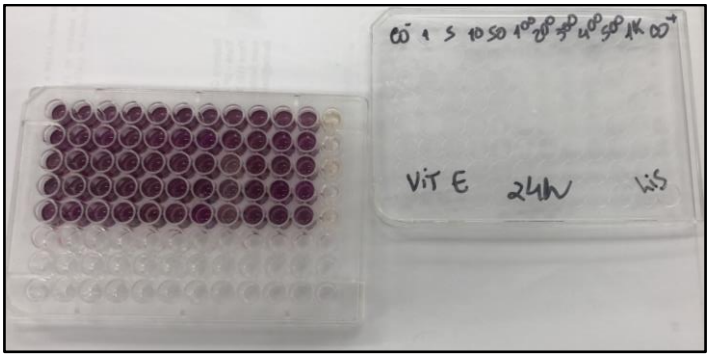

Figure 10 - Plate of NIH3T3 cells with diluted formazan crystals.

The percentage values of cell viability (VC) were estimated by the ratio between the absorbance of the treatment and the absorbance of the negative control, according to Equation 5.

$$VC = \left(\frac{ABS_T}{ABS_{C0-}}\right) \times 100 \quad (5)$$

Where: VC = Cell viability;

ABS_T = Absorbance of the treatment;

ABS_{C0-} = Absorbance of the negative control.

5.3.1.3. Cytoprotection/ Photoprotection test

For the cytoprotection/photoprotection test, three types of treatment were applied: simultaneous, pre-treatment and post-treatment. In the pre-treatment, after the cells had stabilised, they were treated as samples at a concentration of 400 µL.mL-¹ for 2h. After this period, the treatment was removed, set aside, replaced with 20 µL of PBS, and exposed to UVB radiation (60 mJ.cm^{-2}). The reserved treatment was then replaced, and the plates were incubated for 24h.

In the simultaneous treatment, after stabilisation, the supplemented culture medium was removed and replaced with 20 µL of phosphate-buffered saline (PBS). The plates were then exposed to UVB radiation (60 mJ. cm^{-2}) and subsequently treated with the samples (400 µL.mL-¹). After exposure, the cells were incubated for 24h.

Post-treatment, after exposing the cells to UVB radiation (60 mJ. cm^{-2}), the cells were incubated for 2h with a supplemented culture medium and then treated with the samples at a concentration of 400 µL.mL-¹. After treatment, the cells were incubated for 24h.

After 24h of incubation, the culture medium was replaced with a medium containing MTT (0.167 mg.mL-¹) and the plates were incubated for a further four hours. The MTT-

containing medium was then removed and replaced with 100 µL of DMSO to solubilise the formazan crystals. The absorbance was read at 492 nm. The percentage values of VC were estimated by the ratio between the absorbance of the treatment and the absorbance of the negative control, according to Equation 5.

3.5.1.4. Skin corrosion test *in vivo*

The skin corrosion test was carried out according to the methodology of KWAK et al. (2022) with modifications. Five *Eisenia fetida* earthworms were used for each sample. They were washed to remove the soil and then placed on paper towels to remove excess water. Each one was then placed individually in a petri dish (90 x 15 mm) containing filter paper (Whatman no.2) moistened with 2 mL of distilled water.

The test used distilled water (CO-), 0.5 mol hydrochloric acid (CO+) and the samples. These were applied to the worm's skin below the clitellum, with 30 µL of each control solution and the creams being sufficient to cover the clitellum (+/- 34 mg) (MAHMOOD and AKHTAR, 2013).

Afterwards, the Petri dishes were closed with plastic film, and the test units were kept in an incubator (dark, 20 °C). After 2h and 24h, the skin of each worm was observed using a magnifying glass to assess possible changes such as blisters, oedema, corrosion/wear, ulcers, rippling or cuts.

3.5.1.5. Statistical analysis

The absorbance values were subjected to the normality test and analysis of variance (ANOVA) with Dunnett's mean comparison test (α=0.05) for the cytotoxicity tests and Tukey's test (α=0.05) for the cytoprotection tests, using Action Stat software. The number of altered worms and the total number of alterations per worm at each evaluation time in the *in vivo* corrosion test were evaluated. These were subjected to Dunnet's mean comparison test ($p < 0.05$) using the Instat programme.

4. RESULTS AND DISCUSSION

4.1. Development of particle dispersion

Preliminary tests were conducted to define the compounds' methodology and appropriate proportions. Table 1 shows all the methods and compositions used in this work.

Table 1- Preparation composition of all dispersions.

Sample	Ch (%)	CS (%)	References
1.5Ch_1.5CS	1.50	1.50	Sharkawy et al. (2019)
2Ch_2CS	2.00	2.00	Sharkawy et al. (2019)
2_1.5Ch_1.5CS	1.50	1.50	Tan et al. (2018)
3Ch_3CS	3.00	3.00	Tan et al. (2018)
1.6C_25CS	1.60	25.00	Farjado et al. (2010)
1.6Ch_15CS	1.60	15.00	Farjado et al. (2010)
1.6Ch_10CS	1.60	10.00	Farjado et al. (2010)
1.6Ch_5CS	1.60	5.00	Farjado et al. (2010)
0.8Ch_12.5CS	0.80	12.50	Farjado et al. (2010)
0.4Ch_6.25CS	0.40	6.25	Farjado et al. (2010)

All the particles were assessed by DLS, making it possible to obtain D_{43} values, which corresponds to the average particle diameter, calculated as a volume function. Only the average diameter value and the number and volume graphs generated by the software (MASTERSIZER 3000, Manual-2017) were used in this preliminary stage.

The initial methodology was based on the work of SHARKAWY et al. (2019) with adaptations. This study was conducted by the same group as this thesis and established the conditions for producing colloidal particles. In this initial phase, two dispersions were prepared: 1.5Ch_1.5CS containing 1.5% Ch and 1.5% CS, and 2Ch_2CS with 2% Ch and 2% CS. However, the DLS analysis could not be completed for the 1.5Ch_1.5CS and 2Ch_2CS dispersions, as the particles were not detected by the equipment, suggesting that no particles were formed.

The tested second methodology was based on the work of TAN et al. (2018) with adaptations. Two dispersions were prepared in this step: 2_1.5Ch_1.5CS containing 1.5% Ch

and 1.5% CS, and 3Ch_3CS with 3% Ch and 3% CS. Subsequently, the pH of the solutions was adjusted to 3. For this methodology, the DLS analysis did not detect any particles, indicating the absence of particle formation.

The third methodology was based on the work of FARJADO et al. (2010). In this phase, six dispersions were prepared: 1.6Ch_25CS, 1.6Ch_15CS, 1.6Ch_10CS and 1.6Ch_5CS where the four samples contained 1.6% Ch and different concentrations of CS (25%, 15%, 10% and 5%), a dispersion 0.8Ch_12.5CS with 0.8% Ch and 12.5% CS, and 0.4Ch_6.25CS with 0.4% Ch and 6.25% CS. All dispersions showed phase separation and were vigorously stirred to carry out the DLS analysis. Table 2 shows the $D_{4;3}$values of the dispersions.

Table 2- Average particle diameter by volume of the particles' dispersion prepared through the third methodology.

Sample	D_{43} (µm)
1.6Ch_25CS	47.32±1.99
1.6Ch_15CS	15.05±0.95
1.6Ch_10CS	13.65±1.45
1.6Ch_5CS	1.93±0.02
0.8Ch_12.5CS	25.55±0.45
0.4Ch_6.25CS	7.14±2.54

The size of the particles used to prepare Pickering emulsions is one of the parameters that directly influence their stability and the size of the droplets. In general, smaller particles tend to generate more stable emulsions due to faster adsorption kinetics and more efficient packing at the liquid interface (LOW et al., 2020). In this context, Table 2 revealed that sample 1.6Ch_5CS had the smallest average particle diameter of approximately 1.9µm, as well as a reduced average standard deviation, and is, therefore, the sample with the best performance in these parameters. It also revealed that the methodology should continue to be followed in this work.

This result was confirmed by analysing the particle size distribution by number and volume, as shown in Figure 11. The particle size distribution by number indicates how many particles fall within each size range, while the volume distribution shows the total volume

occupied by particles in each size range. Each graph was analysed individually. Sample 1.6Ch_5CS presented narrower and more defined peaks than the other samples, indicating a more uniform particle size distribution. Due to this more consistent distribution, sample 1.6Ch_5CS was selected for further studies.

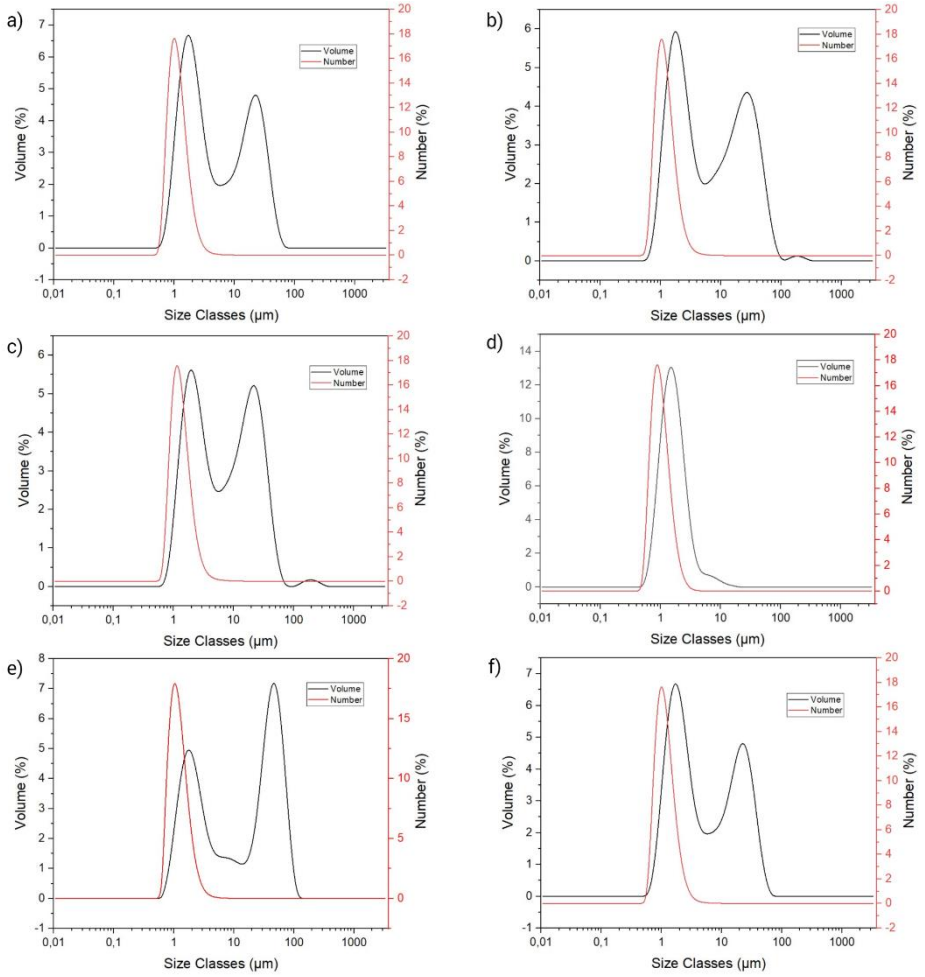

Figure 11 - Graphs of particle size distribution in number and volume for a) 1.6Ch_25CS, b) 1.6Ch_15CS, c) 1.6Ch_10CS, d) 1.6Ch_5CS, e) 0.8Ch_12.5CS and f) 0.4Ch_6.25CS.

Furthermore, based on the preliminary tests carried out, it was possible to observe that varying the concentration of CS significantly altered the size and uniformity of the particles, even influencing the formation of CPs. These changes favoured the production of Pickering particles with more suitable characteristics for stabilising emulsions, ensuring greater efficiency

and stability in formulations. Therefore, the concentration of CS plays a crucial role in controlling particle properties and, consequently, the quality of emulsions.

4.2. Emulsions development

In parallel with particle formulation, the Pickering emulsions were prepared. At this stage, the CI was selected as the evaluation criteria. Two emulsions were prepared with 50% (v/v) Miglyol 812 and 50% (v/v) particle solutions as the aqueous phase (O/W ratio of 50/50) using the methodology of SHARKAWY et al. (2019) (first methodology used). However, the emulsions destabilised immediately after homogenisation. The same happened with the emulsions prepared with the particles following the method from TAN et al. (2018) (second methodology used), which also used the same proportion O/W ratio (50/50) and the same oil. These results are consistent with to the DLS analysis carried out on the preliminary dispersion tests, indicating that the lack of particle formation was the main factor in the non-formation of the emulsions. The lack of suitable particles compromised stabilisation, making it impossible to create a stable interface between the phases, which is essential for emulsification. Figure 12 shows an example of a destabilised emulsion.

Figure 12 - Destabilised emulsion

The particles produced through the third methodology by FARJADO et al. (2010) resulted in phase separation. In this way, two emulsions were made for each dispersion: one using the phase with the highest concentration of particles (bottom) and the other, made after vigorous stirring, to produce Pickering emulsions at a 50/50 O/W ratio as part of an initial screening. Table 3 shows the CI of all the samples over 7 days. Where Ep stands for Pickering emulsion, F1 refers to the lower phase, and F2 refers to using the sample after vigorous stirring. Figure 12 shows an example of an emulsion from this stage.

Table 3- Initial screening of Pickering emulsions production stability by creaming index.

Time (days)	1	5	7
Sample	Creaming index (%)		
EpF1_1.6Ch_25CS	10.00	13.33	13.33
EpF2_1.6Ch_25CS	10.00	13.33	16.67
EpF1_1.6Ch_15CS	10.00	16.67	16.67
EpF2_1.6Ch_5CS	10.00	10.00	16.67
EpF1_1.6Ch_10CS	13.33	16.67	16.67
EpF2_1.6Ch_10CS	16.67	16.67	20.00
Ep1.6Ch_5CS	16.67	16.67	33.33
EpF1_0.8Ch_12.5CS	33.33	33.33	83.33
EpF2_0.4Ch_6.25CS	16.67	16.67	43.33
EpF_12.4Ch_6.25CS	16.67	43.33	83.33
EpF2_0.4Ch_6.25CS	3.33	16.67	43.33

Although Table 3 indicates that the EpF1_1.6Ch_25CS sample showed the best performance over time, as mentioned earlier, the 1.6Ch_5CS dispersion achieved the best results in the preliminary tests. Therefore, even though the Ep1.6Ch_5CS sample did not achieve the best results, it was retained for subsequent tests based on its performance preliminary dispersion test.

After this stage, new emulsions were prepared by varying the oil and dispersions ratio using the Ep1.6Ch_5CS sample. The used ratios included: 40/60 (Ep1.6Ch_5CS40/60), 30/70 (Ep1.6Ch_5CS30/70), 20/80 (Ep1.6Ch_5CS20/80) and 10/90 (Ep1.6Ch_5CS10/90). Table 4 shows the CI of the Pickering emulsions prepared with the dispersion 1.6Ch_5CS.

Table 4- Creaming index of the Pickering emulsions prepared with the 1.6Ch_5CS dispersion.

Time (days)	1	5	7
Sample	Creaming index (%)		
Ep1.6Ch_5CS	16.67	16.67	33.33
Ep1.6Ch_5CS40/6	46.67	50.00	50.00
Ep1.6Ch_5CS30/70	56.67	60.00	60.00
Ep1.6Ch_5CS20/80	60.00	80.00	83.33
Ep1.6Ch_5CS10/90	80.00	83.33	83.33

After analysing the CI of these samples, it was decided to change the study's approach, as these samples also showed inadequate cream formation. It was decided to replace the oil used as the oil phase (dispersed phase) since it can directly influence gravity-induced separation (SHI et al., 2021). Two alternatives were therefore considered: virgin olive oil and sweet almond oil. Two emulsions were then prepared at a 50/50 O/W ratio, one with each oil, and the creaming index of the emulsions was assessed for 30 days. Table 5 shows the creaming index of these emulsions. The EAO1.6Ch_5CS emulsion refers to the emulsion prepared with olive oil, while the EAD1.6Ch_5CS emulsion was made with sweet almond oil. Figure 13 shows the Ep1.6Ch_5CS20/80 sample on day 7.

Figure 13 – Appearance of Ep1.6Ch_5CS20/80 Pickering emulsion at 7 days

Table 5 and Figure 14 show the monitoring of the second stability study in the production of Pickering emulsions by CI, after the oil change.

Table 5- Creaming index - Stability study in the production of Pickering emulsions by creaming index.

Time (days)	1	5	7	30
Sample	Creaming index (%)			
EAO1.6Ch_5CS	6.67	10.00	13.33	16.67
EAD1.6Ch_5CS	33.33	40.00	40.00	36.67

EAO1.6Ch_5CS			
0 days	5 days	7 days	30 days
			
EAD1.6Ch_5CS			
0 days	5 days	7 days	30 days
			

Figure 14 – Creaming index - EAO1.6Ch_5CS and EAD1.6Ch_5CS.

The results shown in Table 5 confirm that the oil change was essential to the success of the formulation. In Pickering emulsion systems, higher viscosity oils are expected to provide better stability, which was also observed in some of the samples in the study by MIKULCOVÁ et al. (2023) and was repeated in this work. Based on the CI of the EAO1.6Ch_5CS sample, it was decided to modify the oil ratio: 10/90, 20/80, 30/70, 40/60, 60/40 and 70/30 as referred to in Table 6, where the CI of the prepared emulsions during 30 days is summarised. Table 6 and Figure 15 shows the monitoring of the third stability study in the production of Pickering emulsions by CI by changing the ratio O/W ratio.

Table 6- Creaming index - Study of the third stability study in the production of Pickering emulsions by creaming index.

Time (days)	1	5	7	30
Sample	Creaming index (%)			
EAO1.6Ch_5CS10/90	76.67	80.00	80.00	80.00
EAO1.6Ch_5CS20/80	36.67	36.67	40.00	40.00
EAO1.6Ch_5CS30/70	10.00	10.00	13.33	13.33
EAO1.6Ch_5CS40/60	3.33	6.67	10.00	10.00
EAO1.6Ch_5CS60/40	0.00	0.00	3.33	3.33
EAO1.6Ch_5CS70/30	0.00	0.00	0.00	0.00

EAO1.6Ch_5CS10/90			
0 days	5 days	7 days	30 days
			
EAO1.6Ch_5CS20/80			
0 days	5 days	7 days	30 days

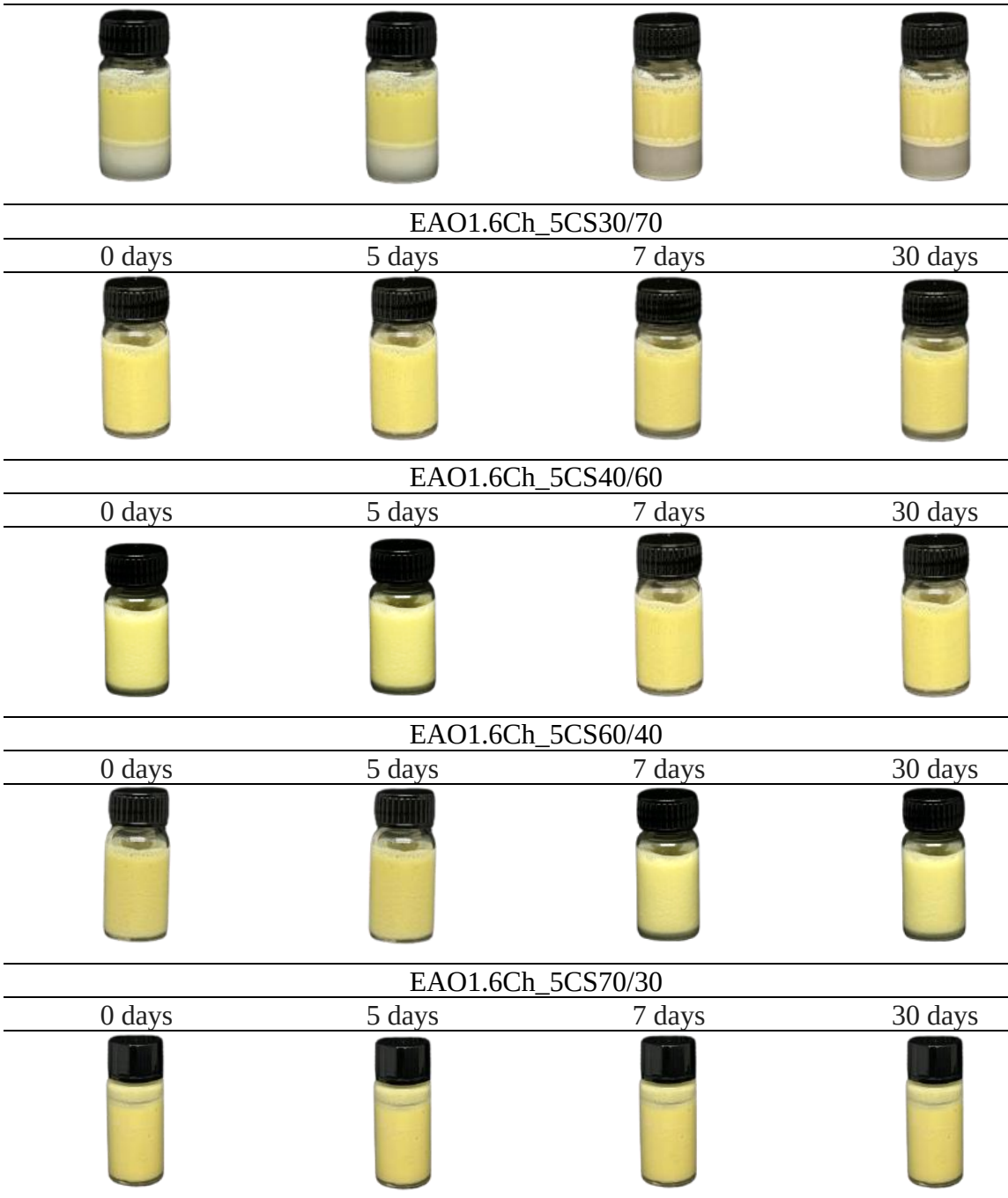

Figure 15 – Creaming index - Study of the third stability study in the production of Pickering emulsions by creaming index.

Based on the results in Table 6 and Figure 15, sample EAO1.6Ch_5CS70/30 showed the best performance among those evaluated. This was the only sample that maintained a CI of 0 throughout the analysis period, indicating excellent stability. Due to its superior behaviour, this sample will be used to develop this work further.

4.3. Development of the formulation for cosmetic applications

4.3.1. Dispersion characterisation

After finalising the preliminary tests, the production of the 1.6Ch_5CS dispersion was repeated. A visual analysis of the particles was carried out after the 24-hour stabilisation period. This analysis showed a change in the turbidity of the sample from translucent to opaque. This change was observed in the reference methodology used after stabilisation as a result of the formation of CPs (FARJADO et al., 2010).

4.3.1.1. Particle size

The size and distribution of the particles were determined using DLS analysis, in which the values of D_{10}, D_{50}, D_{90}, were determined both in volume and number, and $D_{4;3}$ Span, which was determined in volume. The values D_{50} correspond to the median and are defined as the diameter in which half the population is below this value. Similarly, 90% of the distribution is below D_{90}, and 10% is below D_{10}. Span is an indicator of volume uniformity. Table 7 and 8 show the D_{10}, D_{50} and D_{90} values in volume and number, respectively. The $D_{4;3}$ and Span values resulted in values of 1.93 ± 0.02 µm and 1.35 ± 0.01 µm, respectively.

Table 7- Particle size distribution in volume for the sample 1.6Ch_5CS.

Volume	D_{10} (µm)	D_{50} (µm)	D_{90} (µm)
Mean	0.91	1.57	3.02
St Dev	$4.00x10^{-4}$	$1.80x10^{-3}$	0.02
RSD (%)	0.04	0.12	0.55

Table 8 - Particle size distribution in number for the sample 1.6Ch_5C.

Number	D_{10} (µm)	D_{50} (µm)	D_{90} (µm)
Mean	0.66	0.96	1.59
St Dev	$1.00x10^{-4}$	$8.18x10^{-5}$	$2.00x10^{-4}$
RSD (%)	$1.06x10^{-2}$	$8.00x10^{-3}$	0.01

Figure 16 graphically represents the size distribution in volume size and number of the 1.6Ch_5CS sample analysed, which was already presented in Figure 11 on a smaller scale.

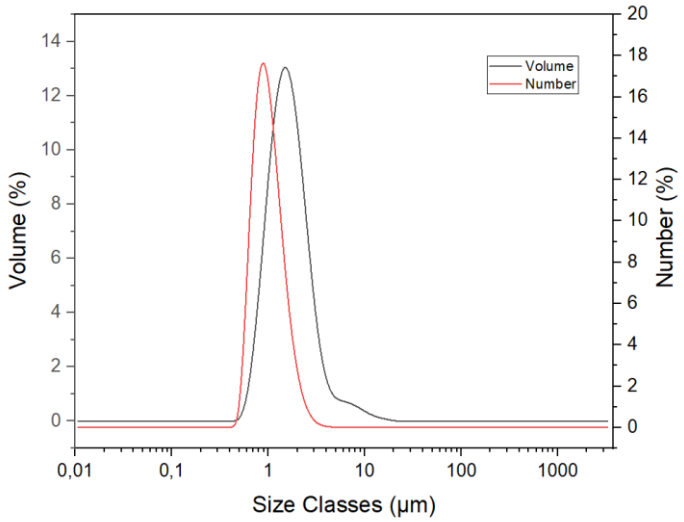

Figure 16- Particle size distribution graph in number and volume sample 1.6Ch_5CS.

The dispersion presented slightly large particles. As mentioned earlier, particle size is directly related to the stability and size of the droplets. Thus, larger particles tend to have slower adsorption and lower packing efficiency at the interface (ALBERT et al., 2019). Several variables that influence the production of the dispersion, such as the solid content, the initial temperature, and the feed flow rate, can influence this behaviour (ZIAEE et al., 2017).

Despite their larger size, microparticles are also widely used as stabilisers, depending on the process variables (MARTO et al., 2016). A practical example can be found in the study by HAN et al. (2024), who developed hydrogel microparticles based on polyethene glycol for stabilising Pickering emulsions. Another relevant example is the work carried out by

BENYAYA et al. (2024), where Pickering emulsions were stabilised by microparticles. This proves the feasibility of using the particles developed in this work.

4.3.1.2. Zeta potential

Charged dispersions can be assessed for stability using ζ, which quantifies the electrostatic repulsion between the particles (GHADIMI et al., 2011; JIANG et al., 2023). Therefore, the greater the stability, the greater the quantity of adsorbed ions and, consequently, the greater the electrostatic repulsion (SMITH et al., 2010). Relatively stable particles are expected to have ζ > 30 mV or ζ < 30 mV (GHADIMI et al., 2011). Sample 1.6Ch_5CS had its ζ measured after the particle stabilisation period, resulting in a value of 32.30 ±1.64 mV, and was considered stable.

The ζ potential is directly related to pH. At lower pHs, Ch shows a high degree of protonation due to the amine groups' protonation, which increases the positive surface charge (ATHAVALE et al., 2022). In this way, the pH of the sample was measured, and a value of 4.6 was obtained, which corroborated its stability.

Two more experiments were carried out to assess the reproducibility of the sample, replicating the same conditions at different times, in addition to the zeta potential measurement mentioned above. The results obtained were 29.06 ±2.01 mV and 31.99 ±0.99 mV, showing a slight and irrelevant variation between the values, confirming the system's stability and consistency.

4.3.1.3. Contact angle

The wettability of the particles is fundamental to determining the capacity to form Pickering emulsions. In this context, the contact angle is a crucial parameter: hydrophilic particles form a θ less than 90°, while hydrophobic particles have a θ greater than 90°. In general, O/W emulsions are stabilised by colloidal particles that form a θ less than 90°, while W/O emulsions are stabilised by particles that form angles greater than 90° (ZHAO, WANG &

ZHANG, 2021). Particles that reach a θ of 90° have a higher stabilising capacity at the emulsion's interface (KAPTAY, 2006). Figure 17 illustrates the droplet record after 30 seconds of analysis.

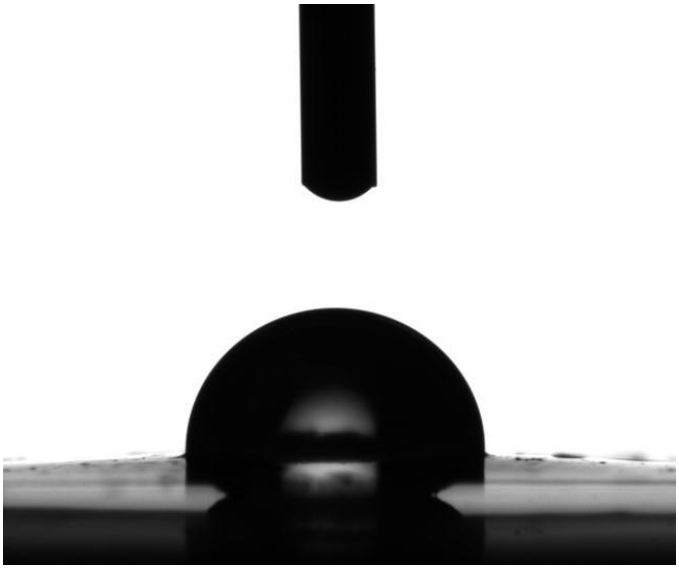

Figure 17 - Contact angle analysis at t=30s.

Based on the data generated by the analysis software, it was quantified that the contact angle of the particles was 97.10 ± 2.91°, classifying them as particles with a hydrophobic character. Despite this angle, in the case of solid particles that form a three-dimensional (3D) network, contact angles of less than 129° and more than 15° can stabilise O/W emulsions, as observed in this study (KAPTAY, 2006; TIAN et al., 2023).

4.3.2. Emulsion characterisation

With the particles, 1.6Ch_5CS, the base emulsion, EAO1.6Ch_5CS70/30 (repeated according to the preliminary tests), and the counterpart added with alpha-tocopherol, VitE1.6Ch_5CS, were prepared. The emulsions were monitored for 30 days, and by visual analysis, the stability of the emulsions was confirmed since phase separation was not observed.

4.3.2.1. Emulsion type

The emulsion type classification was carried out 24 hours after its production. At this stage, a drop of the two emulsions was added to two containers containing oil and deionised water. Figure 18 shows the test of sample b EAO1.6Ch_5CS70/30.

Figure 18 – Droplet test of the emulsion.

As shown in Figure 18, there was no solubilisation in the oil, while solubilisation in the water was appreciated. Thus, the emulsion was classified as O/W, in agreement with the literature (LV et al., 2020). This emulsion type is suitable for applying this work, as O/W emulsions are not oily and are easy to remove from the skin (KHAN et al., 2011).

4.3.2.2. Creaming Index

In general, an emulsion comprises an aqueous phase, an oily phase and a stabiliser. When the emulsion is unstable, the oil droplets rise to the top of the bottle due to their lower density, and the aqueous phase will accumulate at the bottom of the container (KREBS et al., 2013). The CI is a simple visual analysis that considers the height of the formation of the cream, oil, and serum and the phase separation that occurred due to the instability processes (GHIRRO, 2020).

Figure 19 shows the CI of the EAO1.6Ch_5CS70/30 and VitE1.6Ch_5CS emulsions. The results showed stability in both samples over 30 days, indicating a CI% of 0 throughout the analysed period.

EAO1.6Ch_5CS70/30			
0 days	7 days	15 days	30 days
CI=0	CI=0	CI=0	CI=0
			
VitE1.6Ch_5CS			
0 days	7 days	15 days	30 days
CI=0	CI=0	CI=0	CI=0
			

Figure 19 – Creaming index of EAO1.6Ch_5CS70/30 and VitE1.6Ch_5CS samples over 30 days.

As mentioned above, the EAO1.6Ch_5CS70/30 sample had already been analysed previously and showed the same results as those discussed above. This proves the reproducibility of these systems, not only for the dispersion but also for the Pickering

emulsions. From Figures 15 and 19, the reproducibility of the EAO1.6Ch_5CS70/30 sample can be observed, as the sample remained stable on both occasions, displaying a CI of 0.

4.3.2.3. Droplet size

The droplets' size was monitored for 30 days, and the values of D_{10}, D_{50}, D_{90}, $D_{4;3}$, and Span was determined. Table 9 shows the values obtained after the production of the two emulsions.

Table 9– Droplet size of emulsions for the t=0 and t=30.

Parameters	Sample	
	EAO1.6Ch_5CS70/30	VitE1.6Ch_5CS
Time (days)	0	0
D_{10}-V (µm)	12.20 ± 0.13	10.70 ± 0.11
D_{10}- N (µm)	1.15 ± 4.28*10^{-4}	1.15 ± 6.83*10^{-4}
D_{50}- V (µm)	28.30 ± 0.33	24.30 ± 0.34
D_{50}- N (µm)	1.62 ± 1.47*10^{-3}	1.60 ± 2.16*10^{-3}
D_{90}- V (µm)	63.70 ± 1.91	47.40 ± 1.36
D_{90}-N (µm)	3.19 ± 3.89*10^{-3}	3.28 ± 1.44*10^{-3}
$D_{4;3}$ (µm)	34.28 ± 0.49	26.88 ± 0.38
Span (µm)	1.81 ± 0.03	1.29 ± 0.02
Time (days)	30	30
D_{10}-Volume (µm)	12.40 ± 0.262	12.00 ± 0.188
D_{10}- Number (µm)	1.14 ± 4.31*10^{-2}	1.17 ± 3.88*10^{-2}
D_{50}- Volume (µm)	33.7 ± 1.02	31.00 ± 0.74
D_{50}- Number (µm)	1.54 ± 2.87*10^{-2}	1.56 ± 3.2*10^{-2}
D_{90}- Volume (µm)	86.00 ± 5.78	79.8 ± 4.33
D_{90}-Number (µm)	3.06 ± 3.79*10^{-2}	3.14 ± 4.52*10^{-2}
$D_{4;3}$ (µm)	36.38 ± 1.45	33.77 ± 10.94
Span (µm)	1.87 ± 0.53	1.87 ± 0.53

Current literature reports that emulsions should be stabilised by particles of an order of magnitude smaller than the size of the droplet (BINKS & LUMSDON, 2001). Since the dispersion showed $D_{4;3}$ is 1.93 ± 0.02 µm, it was possible to observe that the statement was not confirmed, as very large droplets were not formed. However, other reported works demonstrated that large particles can stabilise an emulsion with droplets of the same size as observed in this work. An example is the work by HE et al. in 2013, where particles with an average diameter of 150 nm formed stable droplets of 450 nm. This may be related to the particle dispersion breaking during the homogenisation period, so it is possible to state that this emulsion would be stabilised indeed by smaller particles (HE et al., 2013; COSSU et al., 2015; ALBERT et al., 2019). Figure 20 graphically shows the size distribution in volume and number of emulsions on the day of production (t=0).

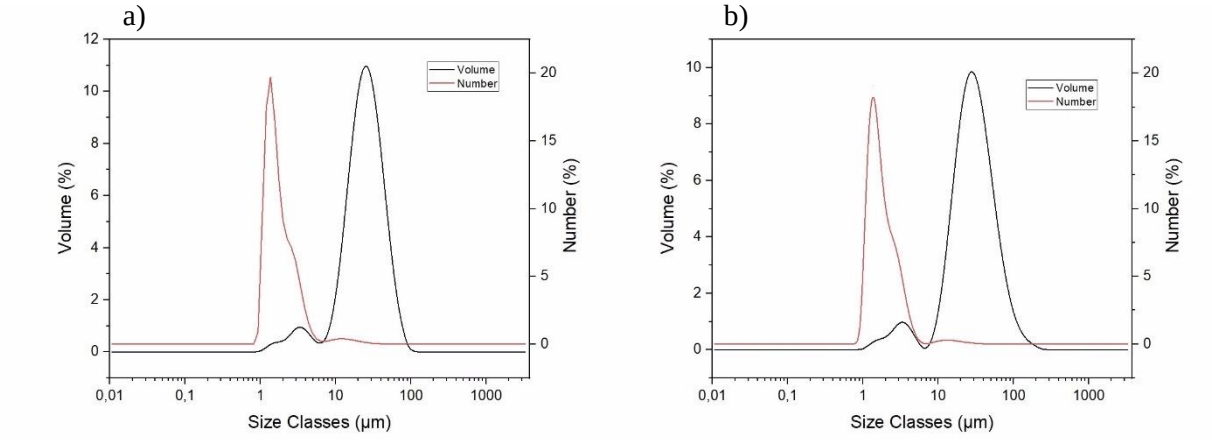

Figure 20- Emulsion droplet size distribution graph in number and volume at t=0 for a) EAO1.6Ch_5CS70/30 and b) VitE1.6Ch_5CS.

The samples presented similar droplet sizes, although the VitE1.6Ch_5CS sample was smaller than the base emulsion. This could be attributed to the vitamin incorporation that could directly affect the surface tension between the oil and water phases and the viscosity of the emulsion, thus reducing the droplets. The same effect occurred in a similar system encapsulating vitamin D3 and curcumin in Pickering emulsions stabilised with lignin particles (ABRAHAM et al., 2024).

DLS analysis was performed thrice at 0, 15 and 30 days to assess the droplets' stability and size. Figure 21 shows the variation in particle volume during the analysis period.

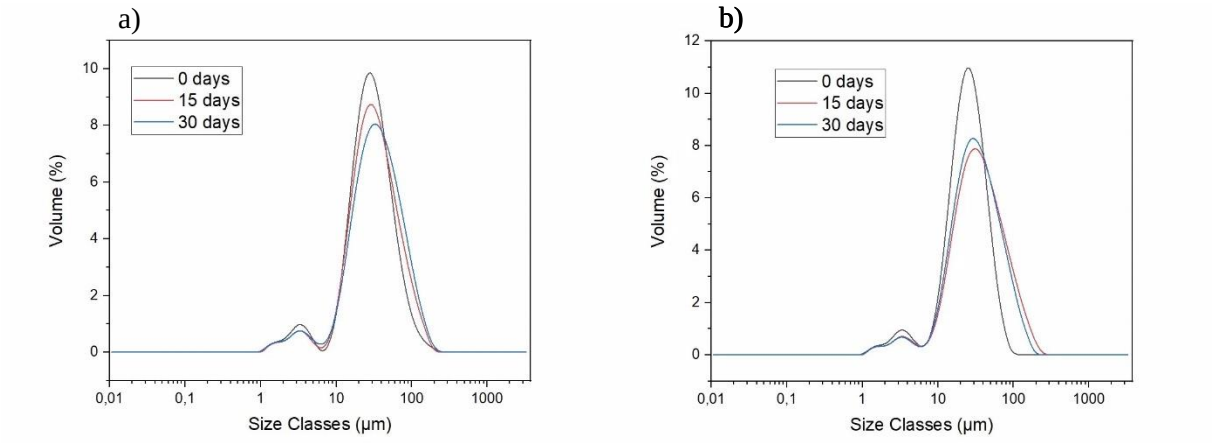

Figure 21- Emulsion droplet distribution graph over one month in volume for a) EAO1.6Ch_5CS70/30 and b) VitE1.6Ch_5CS.

Analysing Figures 20 and 21, it can be seen that there was a slight increase in the droplets of the EAO1.6Ch_5CS70/30 sample, while the VitE1.6Ch_5CS sample showed a higher growth in the emulsion droplets. However, there was no change in the visual aspect of the two emulsions, so it can be concluded that the droplet increase did not influence the stability of the samples.

4.3.2.4. Zeta Potential

The particles' stability can be quantified using ζ, also widely used to characterise emulsions. ζ is an indicator of the intensity of electrostatic repulsion between the droplets. Emulsions with ζ values close to 0 tend to undergo destabilisation processes such as flocculation and coagulation, while those with a high ζ remain electrically stable (LI & XIANG, 2019). Table 10 shows the ζ values of the two samples.

Table 10 – ζ of the emulsions

Sample	EAO1.6Ch_5CS70/30	VitE1.6Ch_5S
Time (days)	ζ (mV)	ζ (mV)
0	38.70 ± 1.33	38.70 ± 1.22
30	42.10 ± 0.57	39.57 ± 0.38

The results confirmed that both samples were within the recommended stability range for emulsions, as far as ζ is concerned. In addition, no significant variation in ζ values was observed over the one-month evaluation period, indicating consistent electrostatic stability during this interval. As in the characterisation of the dispersion, the zeta potential was measured again for the EAO1.6Ch_5CS70/30 sample, recording a value of 35.5±1.23 mV at time zero. There was a slight difference compared to previous measurements, thereby confirming the reproducibility of the sample.

4.3.2.5. Colour test

The colour test results for the two samples are shown in Table 11. In this measurement, the L* values quantify luminosity, ranging from 0 (black) to 100 (white). The a* variable represents the deviation between green and red, being negative (-a*) for green and positive (+a*) for red. The b* values indicate the deviation between blue and yellow, being negative (-b*) for blue and positive (+b*) for yellow (GHIRRO, 2020). The container for liquids was used to measure the emulsions.

Table 11 – Colour test of the emulsions

Sample	EAO1.6Ch_5CS70/30		VitE1.6Ch_5CS	
Parameters	Mean ± Deviation	Cor RGB	Mean ± Deviation	Cor RGB
L*	72.64 ± 0.01		72.43 ± 0.27	
a*	-5.39 ± 0.05		-5.60 ± 0.02	
b*	27.48 ± 0.27		27.35 ± 0.19	

The colour of the emulsions was predominantly light green, which is due to the colour of the oil. The colour of olive oil can vary from yellowish-green to golden, and ripeness is the main interfering parameter (FARIA, 2012). Table 11 shows that the addition of vitamins did not significantly affect the colour of the emulsion.

4.3.2.6. Rheological properties

Static and dynamic rheological properties were assessed to understand the structure of the emulsions. Flow curve tests were determined to analyse the samples' viscosity, varying the shear rate. Figure 22 shows the graph of viscosity variation as a function of the shear rate.

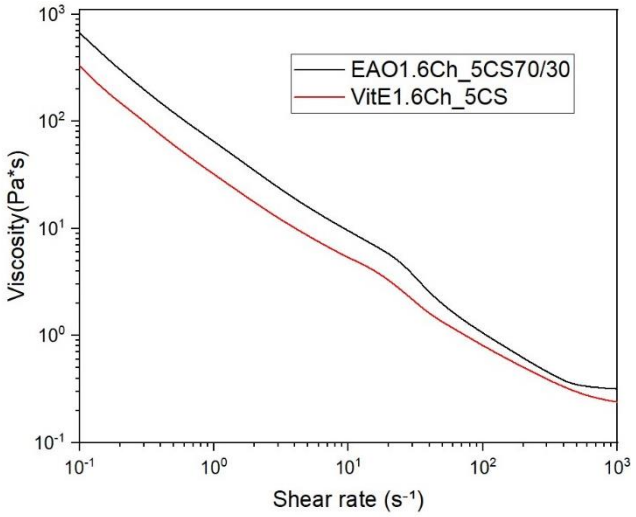

Figure 22- Emulsions' viscosity as a function of the shear rate.

Viscosity quantifies the force of internal friction between the layers of a fluid in motion. As shown in Figure 22, the viscosity of the samples decreased as the applied shear rate increased, showing the typical behaviour of a non-Newtonian fluid. This phenomenon, known as shear thinning, is characteristic of this fluid type. Specifically, pseudoplastic (shear thinning) emulsions are attributed to the breaking or rearranging of the weak droplet network under shear

(HE & LU, 2024). Other studies have presented similar results (TANG et al., 2021). The EAO1.6Ch_5CS70/30 sample presented a higher viscosity, suggesting higher stability since an increase in viscosity can increase strength.

Dynamic oscillation tests under tension were carried out, in which tension is applied gradually at a constant frequency for a given period. This procedure makes measuring the elastic modulus (G‘) and the viscous modulus (G’) possible. In Figure 23, the graph representing these measurements, the breaking point can be identified as the moment when there is a significant change in the behaviour of the moduli, usually indicated by an abrupt decrease in the elastic modulus (G‘), accompanied by an increase in the viscous modulus (G’). This breaking point of the molecular bonds is directly associated with the sample's ability to deform and dissipate heat under mechanical stress, thus reflecting the viscoelastic behaviour of the emulsions (MOURA, 2014).

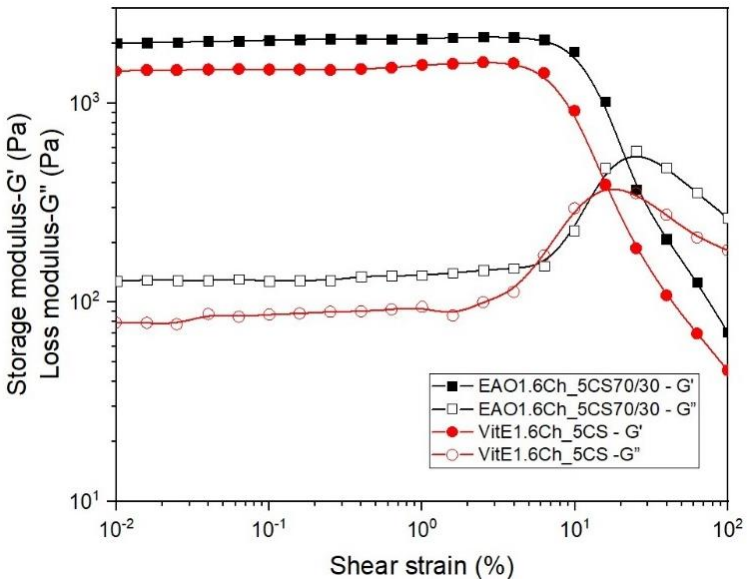

Figure 23- Rheological behaviour of the sample as a function of the shear strain.

The oscillation tests were conducted at a frequency of 0.1 Hz, varying the oscillation amplitude, as observed in Figure 23. When analysing the graph, it is important to highlight two points: the linear viscoelastic region, characterised by the constant behaviour of the G‘ and G” values regardless of the amplitude applied, and the critical deformation point, which marks the transition outside this region. Figure 23 shows this region and that the samples analysed showed

G‘ higher than G” throughout their linear viscoelastic region, indicating that both have a gel-like structure (TANG et al., 2021).

The EAO1.6Ch_5CS70/30 sample showed higher G‘ and G’ values in the linear viscoelastic region than the other samples, suggesting that this emulsion has higher elasticity. In addition, this sample showed a higher critical deformation, which refers to the maximum amount of deformation a material can withstand before suffering permanent deformation or structural failure. This means the emulsion can tolerate higher stress before its internal structure starts to degrade, indicating greater shear strength and a more robust structure. A similar behaviour was observed in Pickering emulsions stabilised with chitosan particles and coated with sodium alginate (TANG et al., 2021).

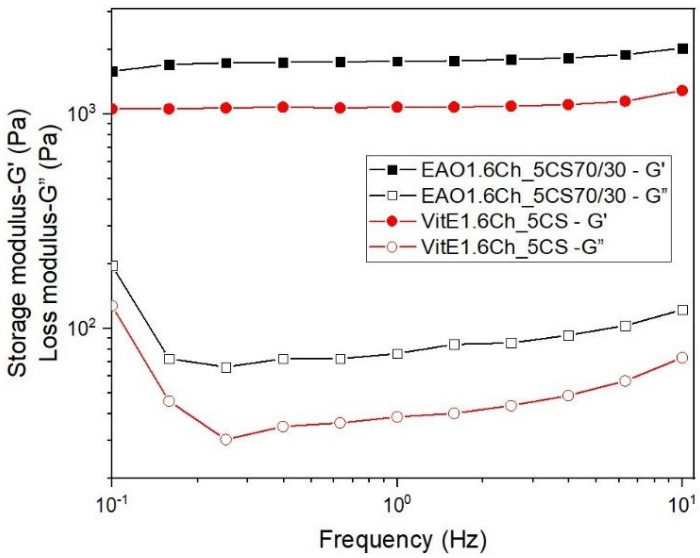

Figure 24- Rheological behaviour of the samples as a function of frequency.

Figure 24 shows the oscillation test results as a function of frequency. For both samples, G‘ was higher than G”, a characteristic of gel behaviour. In addition, the low dependence of the angular frequency for G‘ and G” was observed in both samples, confirming their similarity in forming highly stable gels (TANG et al., 2021).

4.3.2.7. Antioxidant activity

The antioxidant capacity of the VitE1.6Ch_5CS sample was assessed over 30 days using DPPH radical reduction. Figure 25 shows the results obtained for %RSA at 50x, 100x, 500x and 1000x dilutions.

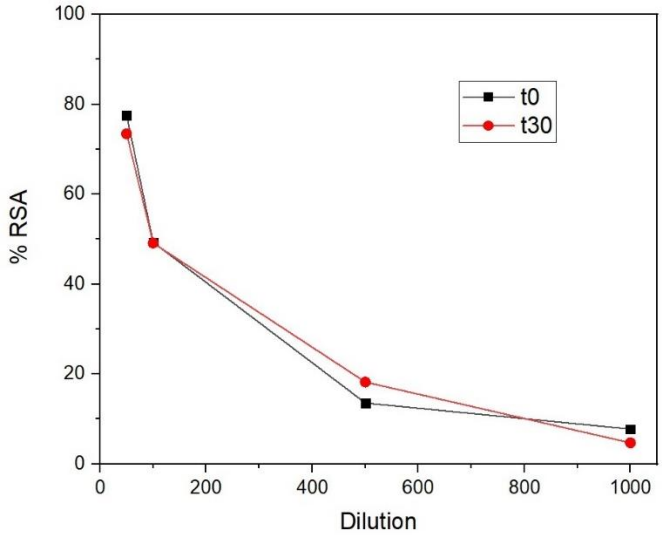

Figure 25- Antioxidant activity expressed as a percentage of radical scavenging activity (%RSA) for the VitE1.6Ch_5CS sample after production (t0) and after 30 days (t30)

The VitE1.6Ch_5CS sample showed a significant antioxidant activity value during the analysis period, indicating its potential for cosmetic application against oxidative stress. The IC_{50} value when the sample was produced (t_0) was $0.02 \pm 2.1*10^{-3}$ (%wt.), and after 30 days (t_{30}) was $0.02 \pm 2.60*10^{-4}$ (%wt.). The average values were the same, demonstrating that the sample did not suffer oxidative stress over time. The results were similar to studies using the same vitamin under the same conditions (SCHREINER et al., 2023).

4.3.2.8. Biologic activity

4.3.2.8.1. Cytotoxicity/Antiproliferative activity

The average absorbance of NIH3T3 cells treated with EAO1.6Ch_5CS70/30 emulsion at concentrations of 400 (24h and 48h) and 500 µL.mL^{-1} (24h) showed statistically higher average absorbance than the CO-. The VC for these concentrations was higher than 124.72%. These results indicate that the EAO1.6Ch_5CS70/30 sample positively affected the viability of the fibroblasts in this study.

The results of the VitE1.6Ch_5CS sample demonstrate that none of the tested concentrations of this emulsion exhibited cytotoxic effects on the cell line. All concentrations at the 24-hour time point displayed mean absorbance values higher than those of the CO-, with percentages VC exceeding 100%. The data show that 400 µL/mL concentration stood out, with the highest viability rates, reaching 165.33% at 24h and 114.19% at 48h, indicating a stimulatory effect on cell division. The concentration of 1000 µL/mL also yielded significant results, with viability of 133.57% at 24 hours and 119.57% at 48h. Table 12 presents the VC results for both samples.

Table 12 - Percentage viability of NIH3T3 cells, MTT test for both samples.

Group/ concentration (µL.mL-¹)	NIH3T3			
	Cell viability (%)			
Sample	EAO1.6Ch_5CS70/30		VitE1.6Ch_5CS	
Time (h)	24	48	24	48
CO-	100.00	100.00	100.00	100.00
CO+	26.07	38.23	43.48	31.06
1	104.68	90.02	151.90	90.85
5	97.06	87.27	134.43	102.05
10	103.37	105.14	154.10	90.46
50	107.18	90.74	151.57	95.65
100	111.98	113.72	147.57	96.43

200	111.11	117.09	144.76	106.96
300	105.16	98.24	124.71	98.10
400	124.72	133.20	165.33	114.19
500	127.34	107.16	151.76	109.36
1000	111.19	107.04	133.57	119.57

CO-: Negative Control; CO+: Positive Control.

Like the EAO1.6Ch_5CS70/30 emulsion, the alpha-tocopherol sample showed no cytotoxic effects at any concentration and demonstrated superior performance compared to the other sample. Figure 26 shows the average absorbance of NIH3T3 cells treated for 24h and 48h with different concentrations of the samples.

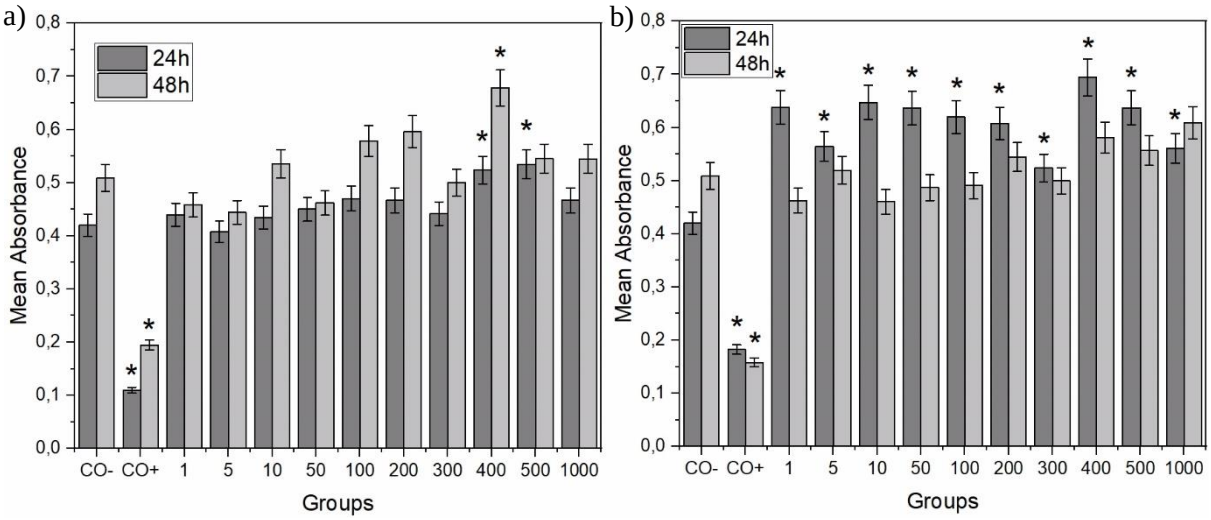

Figure 26- Average absorbance of NIH3T3 cells treated for 24h and 48h with different concentrations for a) EAO1.6Ch_5CS70/30 and b) VitE1.6Ch_5CS.

CO-: Negative Control; CO+: Positive Control.

* Results statistically different from the negative control (Dunnet's test, $p<0.05$).

Several studies have reported similar findings. For instance, SUN et al. (2024) demonstrated that covalent complexes were synthesised to stabilise Pickering emulsions, achieving a VC rate of over 90%, indicating strong biocompatibility and safety. Similarly, in the work of PAN et al. (2024), Pickering emulsions stabilised by nanoparticles composed of

Ampelopsis grossedentata polysaccharide and fish collagen peptide achieved VC values of around 80%. These high VC values (≥80%) confirm the safety of the emulsions and highlight their potential for applications requiring strong biocompatibility.

4.3.2.8.2. Cytoprotection/ Photoprotection test

Initially, the test was carried out on the cells alone, i.e. without treatment with the emulsions, to see how the cells behaved under exposure to radiation. The mean absorbance data of the NIH3T3 cells exposed to the different doses of UVB radiation show that only the lowest concentration evaluated (30 $mJ.cm^{-2}$) at 24h had no cytotoxic effect. The other radiation intensities (60 and 90 $mJ.cm^{-2}$) were cytotoxic at 24h and 48h. Cell viability was even lower than 43.41%, reaching 11.19%. It was possible to observe a reduced viability as time passed and the intensity applied increased. These data confirm that radiation induces a progressive cytotoxic effect, which is more pronounced over more extended periods. Table 13 and Figure 27 show the MTT test VC and the average absorbance of NIH3T3 cells treated with radiation intensities.

Table 13 - Percentage viability of NIH3T3 cells treated with different radiation intensities for 24h and 48h, using the MTT test.

Group/ radiation ($mJ.cm^{-2}$)	NIH3T3	
	Cell viability (%)	
Time (h)	24	48
CO-	100.00	100.00
CO+	24.29	8.50
30	110.26	24.00
60	43.41	14.77
90	31.35	11.19

CO-: Negative Control; CO+: Positive Control.

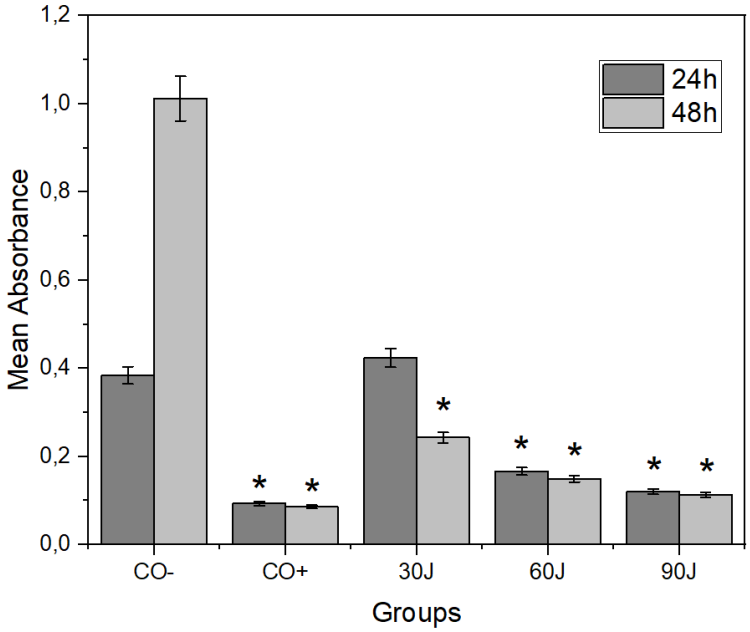

Figure 27- Mean absorbance and standard deviation of NIH3T3 cells treated with radiation intensities for 24h and 48h.

CO-: Negative Control; CO+: Positive Control.

* Results statistically different from the negative control (Dunnet's test, $p<0.05$).

They were considering that 60 mJ. cm^{-2} radiation had a significant cytotoxic effect, with a VC of only 44.95% after 24h; tests were carried out to assess the cytoprotective/photoprotective potential of the emulsions applied. To this end, different ways of applying the creams were tested: simultaneous treatment, pre-treatment and post-treatment, using the samples EAO1.6Ch_5CS70/30 and VitE1.6Ch_5CS, both at a concentration of 400 $\mu L.mL^{-1}$.

Table 14 shows that treatments with the EAO1.6Ch_5CS70/30 and VitE1.6Ch_5CS samples alone demonstrated 94.77% and 93.15% VC, respectively. This suggests that both creams are effective in maintaining cell viability without radiation.

In the simultaneous treatment test, the emulsions showed cell viabilities of 35.46% for EAO1.6Ch_5CS70/30 and 35.46% for VitE1.6Ch_5CS, indicating that the emulsions were unable to protect the cells from the effects of radiation. In the pre-treatment tests, the viabilities were 41.32% for EAO1.6Ch_5CS70/30 and 41.41% for VitE1.6Ch_5CS, which, although higher than the simultaneous treatment, are still lower than the viability observed with radiation

alone. Post-treatment, EAO1.6Ch_5CS70/30 showed 42.26% and VitE1.6Ch_5CS 39.02%, showing that both emulsions have a limited effect in reversing radiation-induced cytotoxicity.

These results indicate that although the emulsions stimulate cell division when applied alone, none of the treatments carried out with radiation managed to improve the VC compared to radiation alone, suggesting that the emulsions did not exert a significant cytoprotective/photoprotective effect under the conditions tested over the 24h. Therefore, a comparison of the results between the simultaneous pre- and post-treatments reveals that, regardless of the mode of application, the emulsions do not achieve the VC observed with the creams applied alone, which was 93.15% 94.77% for EAO1.6Ch_5CS70/30 and 94.15% for VitE1.6Ch_5CS. This suggests that the 60 mJ.cm^{-2} radiation has a predominant cytotoxic effect, which is not sufficiently attenuated by the presence of the emulsions, as seen in Figure 28.

Table 14 – Percentage viability of NIH3T3 cells submitted to treatment with a concentration of 400 μL. mL-1 for the samples and UVB radiation alone and in simultaneous (SIM), pre-treatment (PRE) and post-treatment (POST) cytoprotection/photoprotection treatments.

Group/ radiation/ treatments	NIH3T3
	Cell viability (%)
Time (h)	24
CO-	100.00
CO+	22.91
Radiation (60 mJ. cm^{-2})	44.95
EAO1.6Ch_5CS70/30	94.77
VitE1.6Ch_5CS	93.15
EAO1.6Ch_5CS70/30 SIM	29.08
VitE1.6Ch_5CS SIM	35.46
EAO1.6Ch_5CS70/30 PRE	41.42
VitE1.6Ch_5CS PRE	41.32
EAO1.6Ch_5CS70/30 POST	39.02
VitE1.6Ch_5CS POST	42.26

CO-: Negative Control; CO+: Positive Control.

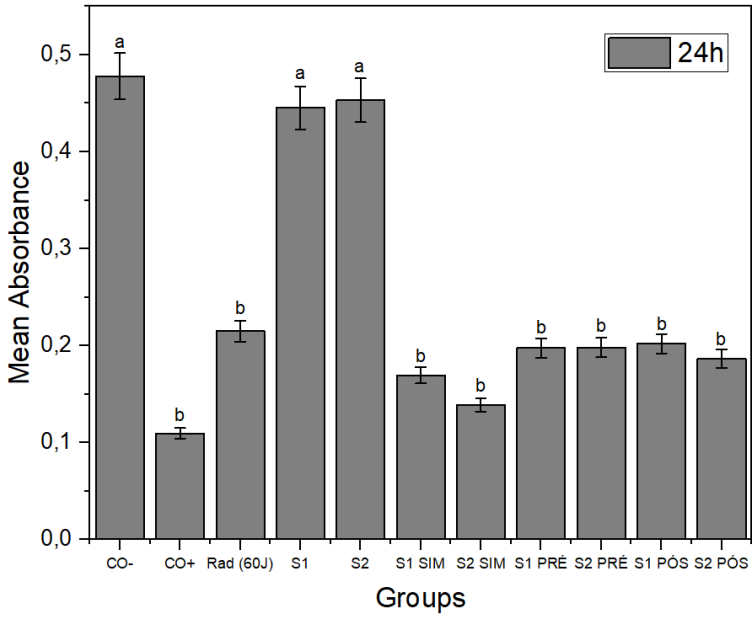

Figure 28 - Mean absorbance and standard deviation of NIH3T3 cells treated with 400 µL. mL^{-1} of the samples and UVB radiation alone and in simultaneous, pre-treatment, and post-treatment cytoprotection/photoprotection treatments.

CO-: Negative Control; CO+; Positive Control; S1: sample EAO1.6Ch_5CS70/30; S2: sample VitE1.6Ch_5CS; Columns followed by the same letter do not differ statistically by the Tukey test ($p<0.05$).

In the study by BORDES et al. (2021), Pickering emulsions stabilised by zinc oxide (ZnO) and titanium dioxide (TiO_2) nanoparticles showed excellent results as sunscreens, demonstrating high efficacy in protecting against UV radiation. The success of these formulations was attributed to the intrinsic ability of ZnO and TiO_2 to absorb and disperse the sun's rays, providing an efficient physical barrier against the damage caused by sun exposure. In contrast, this efficiency was not achieved in the present study because the stabilisers, Ch and CS, do not have the same UV radiation absorption and scattering properties.

4.3.2.8.3. Skin corrosion test *in vivo*

Skin corrosion in earthworms was determined according to the definition of the Globally Harmonised System of Classification and Labelling of Chemicals (GHS) under hazard code

H314, which states that skin corrosion is a hazard that ‘causes severe burns to the skin and damage to the eyes’ (UN, 2021)—considering the irreversible damage to the earthworm's skin, such as blisters, ulcers, oedema, bleeding, thinning, rippling, cutting and mortality.

The results of the corrosion test with the *E. fetida* worms exposed to the EAO1.6Ch_5CS70/30 emulsion and the VitE1.6Ch_5CS emulsion show that neither of them showed an average percentage of worms or an average number of alterations that were statistically different from the CO-, at 2h and 24h. Thus, the data indicate no corrosive effect of the creams on the skin of this organism. Despite this, it was possible to observe blistering, corrosion/wear, oedema and cuts on the skin of the worms exposed to the EAO1.6Ch_5CS70/30 sample and blistering and ulcers on the skin of the worms exposed to the VitE1.6Ch_5CS sample. Figures 29 and 30 show the skins of the earthworms used in this test.

For the positive control, a clear corrosive effect was observed, with the presence of blisters, oedema, corrosion/wear, ulcers and ripples (Figure 31). Within 2h of exposure, 100% of the worms showed some alteration and within 24h, all showed mortality.

Table 15 - Average percentage of worms and an average number of changes in worms exposed to the treatment solutions for 2h and 24 h.

Group/ treatments	Average percentage of altered earthworms (%)		Average number of changes	
Time (h)	2	24	2	24
CO-	0	0	0	0
CO+	100*	100*	3.4*	3.4*
EAO1.6Ch_5CS70/30	20	40	0.4	0.6
VitE1.6Ch_5CS	20	40	0.2	0.6

CO-: Negative Control; CO+: Positive Control.

* Result statistically different from the negative control (Dunnet test, $p < 0.05$).

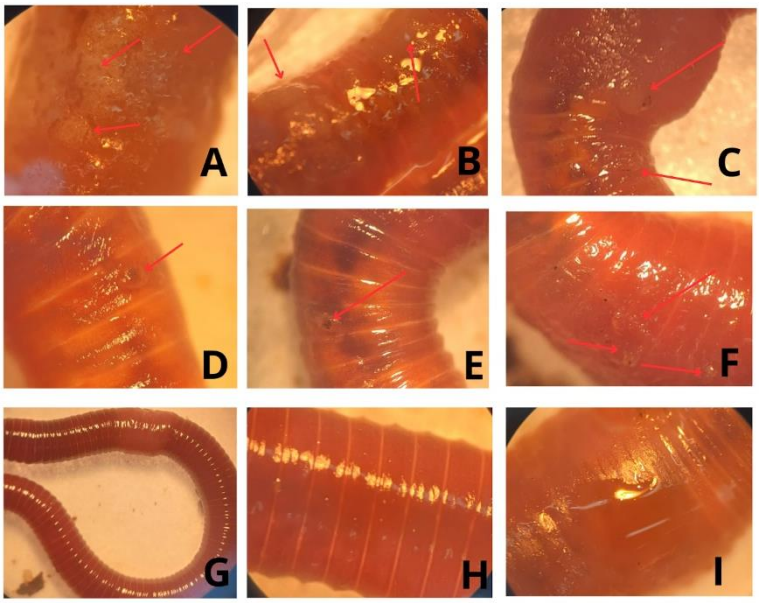

Figure 29- Effect observed under a stereoscopic microscope of sample EAO1.6Ch_5CS70/30 on the organism *E. fetida.*

*Changes observed: A and B - Blisters (2h); C - Blisters and ulcer under the clitellum (24h); D and E - Ulcer (24h); F - Blisters (24h); G and H - No changes; I - clitellum without changes.

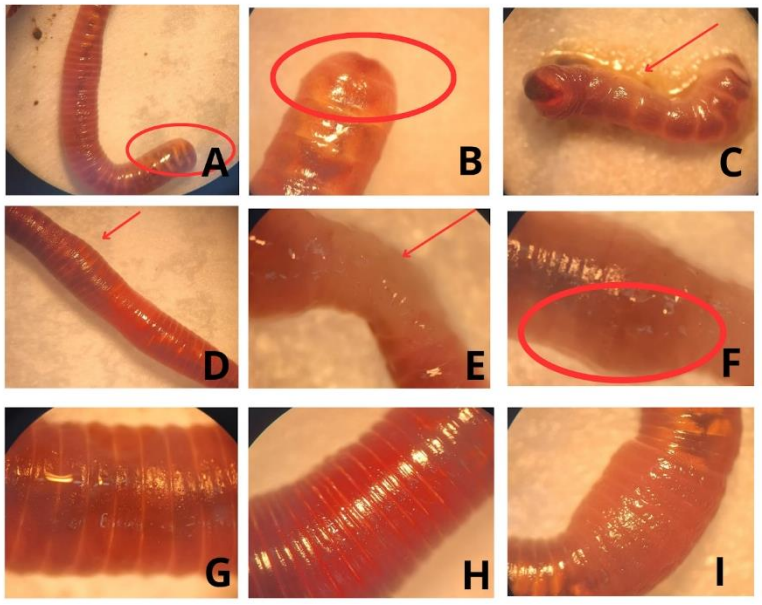

Figure 30- Effect observed under a stereoscopic microscope of sample VitE1.6Ch_5CS on the organism *E. fetida.*

*Changes observed: A and B - Site where the organism was cut (24h); C - Cut (24h); D - Oedema (24 hours); E - Corrosion/wear with blisters (2h);F - Blisters (2h); G and H - No changes; I - clitellum without changes.

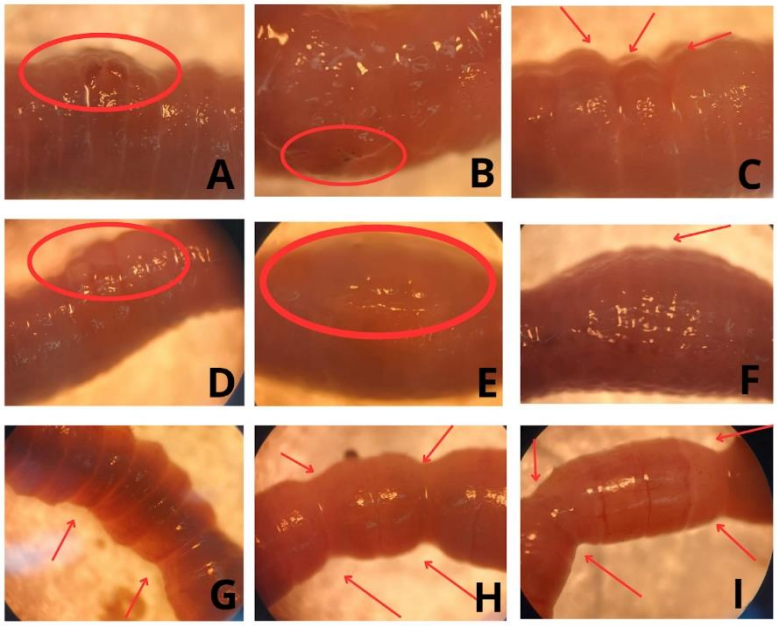

Figure 31- Corrosive effect observed under a stereoscopic microscope of the positive control sample (CO+) on the organism *E. fetida.*

*Changes observed: A and B - Ulcer; C - Ripples; D - Blisters; E - Blisters under the clitellum; F - Oedema; G, H and I - Corrosion/Wear.

In the study by HOU et al. (2024) with *E. fetida*, which assessed the toxicity of aqueous polyurethanes based on castor oil, signs of toxicity similar to those found in this study were also observed. The main symptoms included increased body circumference, haemorrhages, slow movements and the production of a yellowish fluid.

5. CONCLUSIONS

Pickering emulsions have been gaining increasing attention because they are stabilised by solid particles, replacing surfactants or traditional stabilising agents, which can provide products with different characteristics. This study aimed to develop Ch particles incorporating compatible CS to produce Pickering emulsions for topical applications.

Initially, preliminary tests were carried out on the particles' dispersion and the emulsions' preparation. The preliminary dispersion tests resulted in smaller particles than he dispersions made with other proportions made during the preliminary tests, as well as high uniformity. The emulsion tests identified the oil with potential compatibility with the dispersion to develop stable emulsions.

The most promising dispersion (1.6Ch_5CS) was characterised in size, stability and wettability. The particle size and distribution were determined by DLS analysis, with $D_{4;3}$ and Span values of 1.93 ± 0.02 µm and 1.35 ± 0.01 µm, respectively. Despite the slightly large particles, the stability of the emulsion was not compromised.

The ζ measurement was used to assess the charged dispersion's stability. The sample 1.6Ch_5CS showed a ζ value of 32.30 ± 1.64 mV, being considered stable. Wettability was determined by θ, with a value of 97.10 ± 2.91°, indicating a slightly hydrophobic character, suggesting that the particles could stabilise W/O emulsions. However, solid particles that form a three-dimensional network can stabilise O/W emulsions with contact angles between 15° and 129°, as observed in this study.

After the preliminary tests, two emulsions (O/W ratio of 70/30) were prepared: the base EAO1.6Ch_5CS70/30 emulsion and the corresponding formulation added with alpha-tocopherol (VitE1.6Ch_5CS). The emulsions were characterised in terms of droplet size and distribution, morphology, physical stability and antioxidant activity. The emulsion type analysis classified both emulsions as O/W despite the hydrophobic nature of the particles.

The two samples were monitored for 30 days, and the CI analysis indicated no phase separation, indicative of stability. The DLS analysis showed a $D_{4;3}$ of 34.28 ± 0.489 µm for the EAO1.6Ch_5CS70/30 sample and 26.88 ± 0.383 µm for the VitE1.6Ch_5CS sample on day 0, with a slight droplet growth over time, without affecting stability. The ζ led to 38.7 ± 1.326 mV values for the EAO1.6Ch_5CS70/30 and 38.7 ± 1.22 mV for the VitE1.6Ch_5CS samples, confirming stability over time.

The colour test carried out one day after the emulsions' production revealed a light green colour for both. Static and dynamic rheological tests were carried out, indicating the pseudoplastic behaviour of the emulsions in the viscosity analysis. The amplitude and frequency tests revealed characteristics similar to gels. The antioxidant analysis showed high activity on the first day after production, with this activity being maintained throughout the analysed period. Finally, toxicity and cytoprotection tests were carried out and it was possible to verify the absence of toxicity for in vitro fibroblasts and for the skin of worms and absence the sun protection properties of the emulsions for in vitro fibroblasts.

5.1. Future Works

Based on the results obtained and the analyses carried out, it is proposed to continue this work with the following activities:

- Skin permeation tests- These tests will assess the formulation's effectiveness in penetrating the skin layers and determine its bioavailability and therapeutic potential.;
- Antimicrobial tests- These tests will assess the formulation's ability to prevent or combat microbial infections, contributing to its safety and efficacy, especially in dermatological applications;
- Sensorial tests- These will assess sensory characteristics such as texture, odour and general feel on the skin, which are essential parameters for consumer satisfaction and product acceptance;
- Incorporation of other vitamins- Incorporating additional vitamins can increase the multifunctionality of the formulation, offering a more comprehensive range of benefits, such as antioxidant protection or skin moisturisation.

REFERENCES

ABRAHAM, B., et al. Lignin nanoparticles from Ayurvedic industry spent materials: Applications in Pickering emulsions for curcumin and vitamin D3 encapsulation. *Food Chemistry*, 2024, 458: 140284.

ALBERT, C., et al. Pickering emulsions: Preparation processes, key parameters governing their properties and potential for pharmaceutical applications. *Journal of Controlled Release*, 2019, 309: 302-332.

ATHAVALE, R., et al. Tuning the surface charge properties of chitosan nanoparticles. *Materials Letters*, 2022, 308: 131114.

BEDIAKO, J. K., et al. Polyelectrolyte and polyelectrolyte complex-incorporated adsorbents in water and wastewater remediation–A review of recent advances. *Chemosphere*, 2023, 138418.

BELTRÁN C. A. et al., Encapsulação de compostos bioativos por emulsão Pickering: revisão. Revista Colombiana de Investigaciones Agroindustriales, v. 10, 2022.

BENYAYA, M., et al. Rheological properties and stability of Pickering emulsions stabilised with differently charged particles. *Colloids and Surfaces A: Physicochemical and Engineering Aspects*, 2024, 687: 133514.

BINKS, B. P.; LUMSDON, S. O. Pickering emulsions stabilised by monodisperse latex particles: effects of particle size. *Langmuir*, 2001, 17.15: 4540-4547.

BLIX, G.; GARDELL, S. Mucopolysaccharide und Glykoproteide. *Bausteine des Tierkörpers II: Erster Bandteil*, 1960, 662-714.

BORDES, C., et al. Formulation of Pickering emulsions for the development of surfactant-free sunscreen creams. *International Journal of Cosmetic Science*, 2021, 43.4: 432-445.
BOT, A., et al. Emulsion Gels in Food. *Product design and engineering: Formulation of gels and pastes*, 2013.

BRIGGS, N., et al. Stable pickering emulsions using multi-walled carbon nanotubes of varying wettability. *Colloids and Surfaces A: Physicochemical and Engineering Aspects*, 2018, 537: 227-235.

BURGUERA, J. L.; BURGUERA, Marcela. Analytical applications of emulsions and microemulsions. *Talanta*, 2012, 96: 11-20.

CAMPOS, E., et al. Designing polymeric microparticles for biomedical and industrial applications. *European Polymer Journal*, 2013, 49.8: 2005-2021.

CASTRO, R. M. L., et al. Emulsão: uma revisão bibliográfica. 2015.

CHAKRABORTY, G.; BHATTARAI, A.; DE, R. Polyelectrolyte–dye interactions: An overview. *Polymers*, 2022, 14.3: 598.

CHOI, J., et al. Interaction mechanism between low molecular weight chitosan nanofilm and functionalised surfaces in aqueous solutions. *Carbohydrate Polymers*, 2024, 324: 121504.

COSSU, A., et al. Antifungal activity against Candida albicans of starch Pickering emulsion with thymol or amphotericin B in suspension and calcium alginate films. *International journal of pharmaceutics*, 2015, 493.1-2: 233-242.

CUI, F., et al. Polysaccharide-based Pickering emulsions: Formation, stabilisation and applications. *Food Hydrocolloids*, 2021, 119: 106812.

DA SILVA, R. YP, et al. Microparticles in the Development and Improvement of Pharmaceutical Formulations: An Analysis of In Vitro and In Vivo Studies. *International Journal of Molecular Sciences*, 2023, 24.6: 5441.

DE LA CALLE, I., et al. Detection and characterisation of Cu-bearing particles in throughfall samples from vine leaves by DLS, AF4-MALLS (-ICP-MS) and SP-ICP-MS. *Microchemical Journal*, 2017, 133: 293-301.

DOS SANTOS, F. R. A. *Emulsões múltiplas: formulação, caracterização, estabilidade e aplicações*. 2011. PhD Thesis. Universidade Fernando Pessoa (Portugal).

DU, P., et al. Coaxial electrospun TiO2/ZnO core–sheath nanofibers film: Novel structure for photoanode of dye-sensitised solar cells. *Electrochimica Acta*, 2012, 78: 392-397.

DWIPAYANTI, K. S., et al. Enhanced skin localisation of metronidazole using solid lipid microparticles incorporated into polymeric hydrogels for potential improved of rosacea treatment: An ex vivo proof of concept investigation. *International Journal of Pharmaceutics*, 2022, 628: 122327.

FAJARDO, A. R., et al. Time-and pH-dependent self-rearrangement of a swollen polymer network based on polyelectrolytes complexes of chitosan/chondroitin sulfate. *Carbohydrate Polymers*, 2010, 80.3: 934-943.

FARIA, A. S. Q., *Avaliação do efeito da adição de extratos de algas (alga Porphyra umbilicalis e alga Laminaria japónica) na estabilidade de azeite aromatizado*. 2012. Master's Thesis. Instituto Politecnico de Leiria (Portugal).

FENG, X., et al. Effect of oil phases on the stability of myofibrillar protein microgel particles stabilised Pickering emulsions: The leading role of viscosity. *Food Chemistry*, 2023, 413: 135653.

FERREIRA, L. MB; ZUCOLOTTO, V. Chitosan-based nanomedicines: a review of the main challenges for translating the science of polyelectrolyte complexation into innovative pharmaceutical products. *Carbohydrate Polymer Technologies and Applications*, 2024, 100441.

FRISING, T., et al. Contribution of the sedimentation and coalescence mechanisms to the separation of concentrated water-in-oil emulsions. *Journal of Dispersion Science and Technology*, 2008, 29.6: 827-834.

GANGULY, R., et al. Tuning three-dimensional (3D) shapes of polymeric microparticles by geometry-driven control of mold swelling and capillarity in micromolds. *Journal of Colloid and Interface Science*, 2021, 600: 373-381.

GHADIMI, A. et al., A review of nanofluid stability properties and characterisation in stationary conditions. *International journal of heat and mass transfer*, 2011, 54.17-18: 4051-4068.

GHIRRO, L. C. *Desenvolvimento de Emulsões Pickering Para Aplicação Alimentar*. 2019. PhD Thesis. Instituto Politecnico de Braganca (Portugal).

GRAMATGES, A. P. *Nanopartículas de sílica funcionalizadas com grupos amônio e polímeros aniônicos para estabilização de emulsões Pickering contendo repelente de insetos*. 2018. PhD Thesis. PUC-Rio.

HAN, J., et al. Nano-elemental selenium particle developed via supramolecular self-assembly of chondroitin sulfate A and Na2SeO3 to repair cartilage lesions. *Carbohydrate Polymers*, 2023, 121047.

HAN, Y., et al. Enzymatic interfacial conversion of acylglycerols in Pickering emulsions stabilised by hydrogel microparticles. *Journal of Colloid and Interface Science*, 2024, 661: 228-236.

HARVILL, T. L.; HOLVE, D. J. In-process particle size distribution measurements and control. *Particle & particle systems characterisation*, 1993, 10.5: 262-265.

HE, X.; LU, Q.. A review of high internal phase Pickering emulsions: Stabilisation, rheology, and 3D printing application. *Advances in Colloid and Interface Science*, 2024, 103086.

HE, Y., et al. Factors that affect pickering emulsions stabilised by graphene oxide. *ACS applied materials & interfaces*, 2013, 5.11: 4843-4855.

HONG, K.; KIM, S. L., S. B. Effects of HLB value on oil-in-water emulsions: Droplet size, rheological behavior, zeta-potential, and creaming index. *Journal of industrial and engineering chemistry*, 2018, 67: 123-131.

HOU, R., et al. Ecological risk assessment of castor oil based waterborne polyurethane: Mechanism of anionic/cationic state selective toxicity to Eisenia fetida. *Journal of Hazardous Materials*, 2024, 478: 135553.

INDUSTRY PLAZA. Rheometer.. Available at: https://www.anton-paar.com/corp-en/products/group/rheometer/. Accessed on: October 9, 2024.

JAMES-SMITH, M. A.; ALFORD, K.; SHAH, D. O. A novel method to quantify the amount of surfactant at the oil/water interface and to determine total interfacial area of emulsions. *Journal of colloid and interface science*, 2007, 310.2: 590-598.

JARDIM, K. V. Desenvolvimento de nanopartículas de quitosana/sulfato de condroitina para nanoencapsulação da curcumina visando sua liberação controlada e avaliação de sua atividade antitumoral. 2014.

JIANG, Z.; ATILHAN, M; OZBULUT, O E. Exploring optimal dispersion process parameters for fabrication of graphene-reinforced cement composites. *Construction and Building Materials*, 2023, 372: 130805.

KAPTAY, G., On the equation of the maximum capillary pressure induced by solid particles to stabilise emulsions and foams and on the emulsion stability diagrams. *Colloids and Surfaces A: Physicochemical and Engineering Aspects*, 2006, 282: 387-401.

KAWAGUCHI, H. Functional polymer microspheres. *Progress in polymer science*, 2000, 25.8: 1171-1210.

KHAN, B. A., et al. Basics of pharmaceutical emulsions: A review. *African journal of pharmacy and pharmacology*, 2011, 5.25: 2715-2725.

KÖHLER, K., et al. High-pressure emulsification with nano-particles as stabilising agents. *Chemical engineering science*, 2010, 65.10: 2957-2964.

KREBS, T., et al. Coalescence and compression in centrifuged emulsions studied with in situ optical microscopy. *Soft Matter*, 2013, 9.15: 4026-4035.

KWAK, J. I., et al., 2022. Earthworm half-pipe assay: A new alternative in vivo skin corrosion test using invertebrates. Environmental Pollution 307, 119519. https://doi.org/10.1016/j.envpol.2022.119519.

LI, K., et al. Emulsions for enhanced oil Recovery: Progress and prospect. *Journal of Molecular Liquids*, 2023, 123658.

LI, Y.; XIANG, D.. Stability of oil-in-water emulsions performed by ultrasound power or high-pressure homogenisation. *PLoS One*, 2019, 14.3: e0213189.

LIU, Z., et al. Effects of different solid particle sizes on oat protein isolate and pectin particle-stabilised Pickering emulsions and their use as delivery systems. *Food Chemistry*, 2024, 454: 139681.

LOW, L. E., et al. Palm olein-in-water Pickering emulsion stabilised by Fe3O4-cellulose nanocrystal nanocomposites and their responses to pH. *Carbohydrate Polymers*, 2017, 155: 391-399.

LOW, L. E., et al. Recent advances of characterisation techniques for the formation, physical properties and stability of Pickering emulsion. *Advances in colloid and interface science*, 2020, 277: 102117.

LTD, MALVERN INSTRUMENTS. Mastersizer 3000 User Manual. *MANO474*, 2013.

LUNKOV, A. P., et al. Chemical modification of chitosan for developing of new hemostatic materials: A review. *International Journal of Biological Macromolecules*, 2023, 127608.

LV, P., et al. Pickering emulsion gels stabilised by high hydrostatic pressure-induced whey protein isolate gel particles: Characterisation and encapsulation of curcumin. *Food Research International*, 2020, 132: 109032.

MAHMOOD, T., AKHTAR, N., 2013. Short term study of human skin irritation by single application closed patch test: assessment of four multiple emulsion formulations loaded with botanical extracts. Cutan Ocul Toxicol 32, 35–40. https://doi.org/10.3109/15569527.2012.700472.

MALAVAKI, C. J., et al. Capillary electrophoresis for the quality control of chondroitin sulfates in raw materials and formulations. *Analytical biochemistry*, 2008, 374.1: 213-220.

MANGA, M. S., et al. Production of solid-stabilised emulsions through rotational membrane emulsification: influence of particle adsorption kinetics. *Soft Matter*, 2012, 8.5: 1532-1538.

MARTÍNEZ-PALOU, R., et al. Transportation of heavy and extra-heavy crude oil by pipeline: A review. *Journal of petroleum science and engineering*, 2011, 75.3-4: 274-282.

MARTINS, S. P. *Preparação e caracterização de micro/nanopartículas de quitosano para libertação de cisplatina*. 2013. PhD Thesis.

MARTO, J., et al. Pickering emulsions: challenges and opportunities in topical delivery. *Expert opinion on drug delivery*, 2016, 13.8: 1093-1107.

MAYILSWAMY, N.; BONEY, N.; KANDASUBRAMANIAN, B. Fabrication and molecular dynamics studies of layer-by-layer polyelectrolytic films. *European Polymer Journal*, 2022, 163: 110945.

MEKA, V. S., et al. A comprehensive review on polyelectrolyte complexes. *Drug discovery today*, 2017, 22.11: 1697-1706.

MEYER, K. H.; ODIER, M. E.; SIEGRIST, A. E. Constitution de l'acide chondroïtine-sulfurique. *Helvetica Chimica Acta*, 1948, 31.5: 1400-1419.

MIKULCOVÁ, V., et al. On the stabilization of emulsions by cellulose nanocrystals and nanofibrils: Interfacial behavior and synergism. *Colloids and Surfaces A: Physicochemical and Engineering Aspects*, 2023, 675: 131975.

MINAKOV, A. V., et al. Experimental study of the rheological properties and stability of highly-concentrated oil-based emulsions. *Journal of Molecular Liquids*, 2022, 349: 118125.
MORAES, F. P. Alimentos funcionais e nutracêuticos: definições, legislação e benefícios à saúde. *Revista eletrônica de farmácia*, 2006, 3.2.

MORATILLE, Y., et al. Cross-linked polymer microparticles with tunable surface properties by the combination of suspension free radical copolymerisation and Click chemistry. *Journal of Colloid and Interface Science*, 2022, 607: 1687-1698.

MOSMANN, T. Rapid colorimetric assay for cellular growth and survival: Application to proliferation and cytotoxicity assays. Journal of Immunological Methods, dez. 1983. v. 65, n. 1–2, p. 55–63. Available in: <https://linkinghub.elsevier.com/retrieve/pii/0022175983903034>.

MOURA, M. J. C. de. (2014). Preparação e caracterização de hidrogéis de quitosano para administração por via injetável [Tese de Doutoramento]. Universidade de Coimbra.

NIKI, E., Lipid oxidation that is, and is not, inhibited by vitamin E: Consideration about physiological functions of vitamin E. *Free Radical Biology and Medicine*, 2021, 176: 1-15.

NJUGUNA, J.; SACHSE, S. Measurement and sampling techniques for characterisation of airborne nanoparticles released from nano-enhanced products. In: *Health and Environmental Safety of Nanomaterials*. Woodhead Publishing, 2014. p. 78-111.

NOGUCHI, N.; NIKI, E.; Vitamin E nomenclature. Is RRR-α-tocopherol the only vitamin E?. *Free Radical Biology and Medicine*, 2024.

ORTIZ, D. G., et al. Current trends in Pickering emulsions: Particle morphology and applications. *Engineering*, 2020, 6.4: 468-482.

OTTO, D. P.; OTTO, A.; DE VILLIERS, M. M. Differences in physicochemical properties to consider in the design, evaluation and choice between microparticles and nanoparticles for drug delivery. *Expert opinion on drug delivery*, 2015, 12.5: 763-777.

PAN, H., et al. Fabrication, characterisation, and dihydromyricetin-loaded bioavailability of Pickering emulsions stabilised by Ampelopsis grossedentata polysaccharide-fish collagen peptide composite nanoparticles. *Colloids and Surfaces A: Physicochemical and Engineering Aspects*, 2024, 701: 134987.

RAMSDEN, W. Separation of solids in the surface-layers of solutions and ‘suspensions’ (observations on surface-membranes, bubbles, emulsions, and mechanical coagulation) Preliminary account. *Proceedings of the royal Society of London*, 1904, 72.477-486: 156-164.

RANDIVE, R. Application Notes AN011 - Using UV Reflective Materials to Maximise Disinfection - Klaran. 2016. Available in: <https://klaran.com/using-uv-reflective-materials-to-maximize-disinfection>.

ROCHA, D., et al. ALTERNATIVAS AO USO DE MICROPLÁSTICOS NAS INDÚSTRIAS COSMÉTICAS. *Revista Ensaios Pioneiros*, 2020, 4.2: 50-57.

ROSEMAN, S. Reflections on glycobiology. *Journal of Biological Chemistry*, 2001, 276.45: 41527-41542.

SANTOS, C. V. Sulfato de condroitina: da matéria-prima à terapêutica. 2009. *Monografia (Trabalho de Conclusão de Curso em Medicina Veterinária)–Universidade Federal do Rio Grande Do Sul. Faculdade de Veterinária, Porto Alegre*.

SCHIRALDI, C.; CIMINI, D.; DE ROSA, M. Production of chondroitin sulfate and chondroitin. *Applied microbiology and biotechnology*, 2010, 87: 1209-1220.

SCHREINER, T. B., et al. Saponin-based natural nanoemulsions as alpha-tocopherol delivery systems for dermal applications. *Journal of Molecular Liquids*, 2023, 391: 123371.

SHARKAWY, A. et al, Preparation of chitosan/gum Arabic nanoparticles and their use as novel stabilisers in oil/water Pickering emulsions. *Carbohydrate Polymers*, 2019, 224: 115190.

SHARMA, N., et al. Nanoinformatics and biomolecular nanomodeling: a novel move en route for effective cancer treatment. *Environmental Science and Pollution Research*, 2020, 27: 19127-19141.

SMITH, R. J. et al., The importance of repulsive potential barriers for the dispersion of graphene using surfactants. *New Journal of Physics*, 2010, 12.12: 125008.

SU, S., et al. Novel concentrated O/W emulsion co-stabilised by like-charged chitosan nanoparticle and ethyl lauroyl arginate (LAE) surfactant at very low dosages. *LWT*, 2024, 191: 115692.

SUN, G., et al. Preparation of uniform particle-stabilised emulsions using SPG membrane emulsification. *Langmuir*, 2014, 30.24: 7052-7056.

SUN, Y., et al. Preparation and characterisation of lactoferrin-polyphenol conjugate with stabilising effects on fish oil high internal phase Pickering emulsions. *Food Chemistry: X*, 2024, 101836.

TAN, C et al., Anthocyanin stabilisation by chitosan-chondroitin sulfate polyelectrolyte complexation integrating catechin co-pigmentation. *Carbohydrate polymers*, 2018, 181: 124-131.

TANG, Y., et al. The microstructure and physiochemical stability of Pickering emulsions stabilised by chitosan particles coating with sodium alginate: Influence of the ratio between chitosan and sodium alginate. *International Journal of Biological Macromolecules*, 2021, 183: 1402-1409.

TERESCENCO, D., et al. Influence of the emollient structure on the properties of cosmetic emulsion containing lamellar liquid crystals. *Colloids and Surfaces A: Physicochemical and Engineering Aspects*, 2018, 536: 10-19.

THOMPSON, K. L.; ARMES, S. P.; YORK, D. W. Preparation of pickering emulsions and colloidosomes with relatively narrow size distributions by stirred cell membrane emulsification. *Langmuir*, 2011, 27.6: 2357-2363.]

TOPAN, J. F. *Emulsões à base de óleo de girassol (Helianthus annus L.) com cristal líquido: avaliação das propriedades físico-químicas e atividade cosmética*. 2012. PhD Thesis. Universidade de São Paulo.

UN, 2021. Gobally Harmonized System of Classification and Labelling of Chemi Cals (GHS), in: Ninth Revised Edition. United Nations, New York and Geneva. Ninth revised edition. United Nations, New York and Geneva., p. 255.

WANG, S., et al. Chitosan-based food-grade Pickering emulsion loading with Rosa roxburghii extract against precancerous lesions of gastric carcinoma. *International Journal of Biological Macromolecules*, 2024, 258: 128093.

WANG, Y., et al. Conformational changes and the formation of new bonds achieving robust nanoemulsions by electrostatic interactions between whey protein isolate and chondroitin sulfate. *Food Hydrocolloids*, 2023, 136: 108263.

YANG, Y.; MCCLEMENTS, D. J., Encapsulation of vitamin E in edible emulsions fabricated using a natural surfactant. *Food Hydrocolloids*, 2013, 30.2: 712-720.

YUAN, Q., et al. Enhancing the throughput of membrane emulsification techniques to manufacture functional particles. *Industrial & engineering chemistry research*, 2009, 48.19: 8872-8880.

YUAN, Y., et al. Fabrication of stable zein nanoparticles by chondroitin sulfate deposition based on antisolvent precipitation method. *International journal of biological macromolecules*, 2019, 139: 30-39.

ZANOTTI, M. A. G. Propriedades de emulsões óleo em água formuladas com emulsificantes reconfiguráveis através de alterações no PH. 2017.

ZHANG, G., et al. Evolutionary mechanism and particle characterisation analysis of dust produced by wet-mix shotcrete in tunnels. *Construction and Building Materials*, 2024, 411: 134375.

ZHAO, H., et al. Pickering emulsion stabilised by dual stabiliser: a novel reaction/separation system for methacrolein synthesis. *Chemical Engineering Science*, 2021, 229: 116038.

ZHU, X., et al. Tuning complexation of carboxymethyl cellulose/cationic chitosan to stabilise Pickering emulsion for curcumin encapsulation. *Food Hydrocolloids*, 2021, 110: 106135.

ZIAEE, A., et al. (2017). Spray drying ternary amorphous solid dispersions of ibuprofen–An investigation into critical formulation and processing parameters. European Journal of Pharmaceutics and Biopharmaceutics, 120, 43-51. https://doi.org/10.1016/j.ejpb.2017.08.005.